


Spring 2019

Evaluating the Effects of Antibody-Conjugated Multi-Walled Carbon Nanotubes in Combination with Microwave Irradiation

Amy Chall

Follow this and additional works at: <https://digitalcommons.georgiasouthern.edu/etd>

 Part of the [Animal Experimentation and Research Commons](#), [Cancer Biology Commons](#), [Immunopathology Commons](#), [Medicinal Chemistry and Pharmaceutics Commons](#), [Nanomedicine Commons](#), [Oncology Commons](#), and the [Pathology Commons](#)

Recommended Citation

Chall, Amy, "Evaluating the Effects of Antibody-Conjugated Multi-Walled Carbon Nanotubes in Combination with Microwave Irradiation" (2019). *Electronic Theses and Dissertations*. 1913.
<https://digitalcommons.georgiasouthern.edu/etd/1913>

This thesis (open access) is brought to you for free and open access by the Graduate Studies, Jack N. Averitt College of at Digital Commons@Georgia Southern. It has been accepted for inclusion in Electronic Theses and Dissertations by an authorized administrator of Digital Commons@Georgia Southern. For more information, please contact digitalcommons@georgiasouthern.edu.

EVALUATING THE EFFECTS OF ANTIBODY-CONJUGATED MULTI-WALLED CARBON
NANOTUBES IN COMBINATION WITH MICROWAVE IRRADIATION

by

AMY FRAZIER CHALL

Under the Direction of Vinoth Sittaramane

ABSTRACT

Cancer remains one of the largest public health concerns of our day, particularly in developed countries where technological advances have allowed populations to live well into their eighth decade. In America, those in their 80's have a 1 in 2 chance of developing cancer in their lifetime. Prostate cancer, specifically is the second leading cause of cancer deaths in males. Traditional cancer therapies cause high levels of toxicity to the patient due to mechanisms of action that often attack cancer cells and healthy cells alike. The holy grail of cancer research is to find a treatment that targets the cancer cell directly while leaving healthy cells unharmed. The introduction of monoclonal antibodies as a way to target antigens that are highly expressed on cancer cells may be one way to reach this goal. Coupling antibodies with nanomaterials has also shown promising results which is the subject of this study. Multi-walled carbon nanotubes (MWCNT) possess the unique ability to be rapidly heated under microwave irradiation. Furthermore, the sidewalls can be modified to attach various molecules and proteins to its surface. This study evaluated MWCNTs conjugated with an antibody directed against prostate specific membrane antigen (PSMA) in combination with microwave irradiation as a potential ablative therapy. This study demonstrates hyperthermic ablation of the muscle cells surrounding antibody-conjugated MWCNTs after microwave irradiation. Additionally, it showed that these nanotubes remain localized at the sight of injection with no evidence of distribution amongst other tissue. Time-lapse confocal microscopy using transgenic zebrafish larvae demonstrated that macrophages and neutrophils are the first immune responders with phagocytosis. These findings support further efficacy studies in a human prostate tumor xenograft mouse model.

INDEX WORDS: Nanomedicine, Hyperthermic necrosis, Innate immunity, Mice, Zebrafish, Prostate specific membrane antigen, Neutrophil, Macrophage, Histopathology

EVALUATING THE EFFECTS OF ANTIBODY-CONJUGATED MULTI-WALLED CARBON
NANOTUBES IN COMBINATION WITH MICROWAVE IRRADIATION

by

AMY FRAZIER CHALL

B.S., Austin Peay State University, 2009

A Thesis Submitted to the Graduate Faculty of Georgia Southern University in Partial
Fulfillment of the Requirements for the Degree

MASTER OF SCIENCE

STATESBORO, GA

© 2019

AMY FRAZIER CHALL

All Rights Reserved

EVALUATING THE EFFECTS OF ANTIBODY-CONJUGATED MULTI-WALLED CARBON
NANOTUBES IN COMBINATION WITH MICROWAVE IRRADIATION

by

AMY FRAZIER CHALL

Major Professor:
Committee:

Vinoth Sittaramane
Dongyu Jia
Rafael Quirino
W. Eric Gato

Electronic Version Approved:

May 2019

DEDICATION

I dedicate this work to my children.

You are the reason I wanted to give up. But most importantly, you are the reason I never did.

ACKNOWLEDGMENTS

I would like to first acknowledge my advisor, Dr. Vinoth Sittarmane. Thank you for taking the time to teach me the ins and outs of research. I'd also like to acknowledge the hard work of everyone in the Chemistry Department at Georgia Southern University, including Dr. Rafael Quirino, Dr. Eric Gato, Andrew Mixson, John Stagg, and Moses Kusi. A big thanks is due to Craig Banks with the Biology Department Fieldhouse for his help with the mice. I would like to show gratitude to Andrew Diamanduros for his unlimited availability when I needed help with the confocal microscope. I'd also like to thank Dr. Ray Chandler for helping me work through my statistical conundrums. Finally, I would like to thank all of my coworkers, friends, and family who have been there through the highs and the lows. I could write another 50 page thesis just describing what your support means to me.

TABLE OF CONTENTS

	Page
ACKNOWLEDGMENTS	3
LIST OF TABLES	5
LIST OF FIGURES.....	6
CHAPTER	
1 INTRODUCTION.....	7
I. Cancer Background.....	7
II. Current Therapies	7
III. Purpose of the Study	20
2 MATERIALS AND METHODS	24
I. Preparation of Antibody Conjugated Carbon Nanotubes.....	24
II. Microwave Irradiation Optimization.....	25
III. Mice	26
IV. Mice Experimental and Control Groups.....	27
V. Anesthesia	28
VI. Intramuscular Injection of Carbon Nanotubes.....	29
VII. Microwave Irradiation	29
VIII. Euthanasia	29
IX. Tissue Preparation.....	30
X. Slide Analysis.....	30
XI. Zebrafish Embryo Model.....	30
XII. Confocal Fluorescent Microscopy and Time-Lapse Imaging.....	31
XIII. Statistical Analysis.....	31
3 RESULTS AND DISCUSSION.....	32
I. Antibodies are Effectively Conjugated to MWCNTs.....	32
II. Microwave Irradiation Optimization.....	33
III. Necrosis was Observed at the Site of MWCNT Injection.....	33
IV. MWCNTs are not Evident in the Vital Organs.....	39
V. Neutrophils and Macrophages Experience Frustrated Phagocytosis in Zebrafish.....	41
VI. Effects of Microwave Irradiation on mice.....	45
4 CONCLUSION.....	48
I. A Novel Therapy.....	48
II. Further Evaluation of Results.....	49
III. Further Modifications of MWCNTs.....	50
IV. Conclusion	51
REFERENCES	53

LIST OF TABLES

	Page
Table 1: Biodistribution of CNTs.....	17
Table 2: Microwave optimization schedule.....	26
Table 3: Mice experimental and control groups.....	28
Table 4-A: χ^2 values comparing hyperthermic necrosis frequencies between groups sacrificed 24 hours post-treatment.....	35
Table 4-B: χ^2 values comparing hyperthermic necrosis frequencies between groups sacrificed 1 week post-treatment	35
Table 4-C: χ^2 values comparing hyperthermic necrosis frequencies between groups sacrificed 2 weeks post-treatment.....	35
Table 4-D: χ^2 values comparing hyperthermic necrosis frequencies between groups sacrificed at all time-points combined	36

LIST OF FIGURES

	Page
Figure 1: Physical representation of carbon nanotubes.....	13
Figure 2: Preparation of antibody-conjugated MWCNTs.....	25
Figure 3: Milestone Ethos Synth 1600 URM Microwave Labstation with control unit	25
Figure 4: Demonstration of intramuscular injection.....	29
Figure 5: Analysis of antibody conjugation.....	32
Figure 6: Power optimization trials.....	33
Figure 7: Histology demonstrating types of necrosis.....	34
Figure 8: Histology demonstrating necrosis in treatment groups.....	36
Figure 9: Histology demonstrating decreased inflammation over time.....	39
Figure 10: Histology demonstrating organ biodistribution.....	41
Figure 11: <i>Tg(mpx1::gfp)</i> zebrafish embryos demonstrating neutrophilic infiltration specific to ab-MWCNT presence.....	42
Figure 12: Time-lapse demonstrating neutrophil recruitment.....	43
Figure 13: Time-lapse demonstrating attempted macrophage phagocytosis.....	44
Figure 14: Microwave-induced lesions in mice.....	46
Figure 15: Mouse positioning for microwave irradiation.....	46

CHAPTER 1

INTRODUCTION

I. Cancer Background

Cancer remains one of the largest public health concerns of the 21st century. In 2018, more than 8 million people lost their lives to cancer worldwide. While cancer is certainly associated with certain risk factors such as carcinogen exposure, viruses, and genetics, it is largely associated with the aging process. Technological advances over the last century allow populations in the developed world to survive well into their eighth decade and beyond. Therefore, as the risk of death due to injury or acute infection decreases, the likelihood that one will succumb to diseases of aging increases. Essentially, if one lives long enough, they will likely encounter a neoplasm simply as a function of age. In fact in America, those who live into their 80's have a 1 in 2 chance of developing cancer in their lifetime. For adult males, this often comes in the form of prostate cancer ¹. As the aging population grows alongside increased exposure to carcinogens, it is projected that the global economic burden of cancer will continue to rise along with the annual number of cancer deaths from 8.2 million to 13 million over the next 20 years ². The U.S. federal funding alone for cancer research was \$305 million in 2018 ³. The race is on to build upon the scientific understanding of what causes cancer and develop new therapies to combat this growing epidemic.

II. Current Therapies

From the beginning, researchers have been on a quest to find drugs that are potent enough to kill tumor cells while sparing the life of the patient. This has been a delicate balancing act, as many of the first line anti-cancer regimens available today are still highly toxic to the patient. Side effects commonly associated with current therapies range from benign hair loss to acute myelosuppression, which put patients at risk of succumbing to life-threatening infections. Investigations into the etiology of cancer in the last seventy years have translated into therapies that have drastically decreased the mortality of cancer patients

². The research that has led to breakthroughs in developing new treatments has also illuminated the scope of the problem. Much like the Greek mythology of Heracles and Hydra, the more science learns about the mechanisms of cancer, the more it becomes clear that this tiny killer is a monster of complexity and single therapies alone only slay a small fraction of the beast. A multi-pronged approach that severs many heads is required to eradicate cancer. Today, clinical treatment of cancer often involves a combination of several of the following anti-cancer elements:

Chemotherapy

The use of nitrogen mustard for the treatment of lymphoma in 1949 emerged following World War II when physicians noted a marked decrease in blood cell development in soldiers returning from the war. It was discovered that the use also halted cell proliferation in lymphoma patients. It is now known that this drug and its derivatives kill cancer cells through DNA alkylation. During cell replication, DNA is exposed and damaged by these agents. Cancer cell populations rapidly divide and proliferate, thus making them particularly vulnerable to this agent. However, treatment with this chemotherapy alone results in only short-lived remission. A class of drugs called antifolates emerged in the 1950's with the leading drug, methotrexate, still in use today. This class also targets DNA synthesis, but by interfering with folate, a necessary co-factor in the process ⁴. However, these two classes of drugs have serious drawbacks. They exhibit a low therapeutic index when used alone as they do not distinguish between cancerous and healthy dividing cells. Therefore, they must be used near their maximum tolerated dose to achieve an effect which can result in morbidity and mortality associated with the therapies themselves ⁵. Furthermore, alkylating agents boast a higher rate of causing subsequent neoplasms; as one tumor is cured, another may develop later as a direct result of the therapy ⁶.

Second generation drugs evolved alongside progress in the field of molecular genomics. These allow for a more tailored approach by targeting specific cell signaling events that result due to specific gene mutations. For example, the BCR/ABL fusion gene results during a chromosomal recombination that leads to Chronic Myelogenous Leukemia (CML). The resulting fusion gene then

increases the activity of tyrosine kinase in the affected cells, leading to a net increase in proliferative activity. Tyrosine kinase inhibitors have been very effective at treating CML positive for this fusion gene and prolonging life. Unfortunately, the heterogenic nature of malignancy often means that not all cancerous cells contain the targeted mutation, making them insusceptible to targeted treatments which can result in drug resistance ⁴.

Radiation Based Therapies

The first therapy to use radioactivity traces back to the late 1800's when X-rays were first used to treat forms of skin cancer. The discovery of radioactive elements and the description of its physiological effects by Marie and Pierre Curie led to its use as an anti-cancer therapy. Similarly to first generation chemotherapies, the mode of action targets the DNA replicating machinery of the cell and limits its ability to divide. Unsurprisingly, this often leads to considerable injury to healthy tissue as well. Technological advances have eventually led to the development of X-rays capable of penetrating deeper tissues and dose administration schedules that have decreased the toxicity to healthy cells ⁷.

Hyperthermic Ablation

Hyperthermic ablation, or the use of heat to achieve cell death, is another approach to treating cancer ⁸. This may be the oldest therapy, with Hippocrates being said to have cauterized the superficial tumors of his patients. Modern applications did not emerge until the 1970's. These techniques involve the application of energy through a probe which is then absorbed by the tissue in the form of heat. This energy can be delivered across various wavelengths in the form of radiofrequency (RF), microwave, and light lasers. Light lasers are by far the most commonly used mode of hyperthermic ablation for superficial tumors, though insertion of optical probes has been used for bladder and uterine cancers. It consists of the delivery of a wide range of light wavelengths depending on the target tissue that is delivered through a medium. Many factors are taken into consideration when applying this therapy, but altering the wavelength and the diameter of the medium allows for penetration at different depths, making this a

versatile tool that can be tailored to different cancers. For example, infrared light is absorbed best when deeper penetration is required, whereas superficial malignancies require a higher wavelength. Radiofrequency ablation induces hyperthermia through a different mechanism. Radio waves transmit electricity through the tissue between two probes. The electrical energy is absorbed as heat. It is used more commonly to treat deeper cancers, particularly hepatic colorectal malignancies. One drawback has been its tendency to produce asymmetric ablation patterns. This is because the energy tends to move through areas of the tumor with less resistance. Microwave ablation, however, heats through an entirely different mechanism known as the Joule effect, where the energy from microwaves causes rapid oscillation of water molecules resulting in friction which is then transferred as heat. This allows a deeper penetration superior to both light and radiofrequency application ⁹. Microwaves are currently being used clinically as part of a combination therapy to shrink tumors in the lungs and liver ¹⁰⁻¹³.

Immunotherapy

The advent of monoclonal antibodies in the 1970's allowed for the possibility of making current therapies more targeted to the cancer cell. Monoclonal antibodies are produced using hybridoma technology and are tailored to bind to specific antigenic epitopes with high affinity and can be designed to target specific antigens that are highly expressed on cancer cells. The antibody-antigen interaction then serves to either block or activate cell signaling events that eventually result in the cancer cell's demise. They also serve to opsonize the targeted cell, making them a target for the patient's own immune system to attack ¹⁴. It has become standard to use monoclonal antibodies in combination with chemotherapeutic agents in the treatment of certain breast cancers, colorectal cancers, and non-Hodgkin's lymphoma ⁴. More recently, these antibodies have been used as a way to target chemotherapy directly to cancer cells by directly attaching the drug to the antibody. These antibody-drug conjugates (ADC) can then shuttle the payload to the tumor and facilitate uptake into the cell by harnessing receptor mediated endocytosis. Brentuximab Vedotin, is an ADC that has demonstrated success in the treatment of anaplastic large-cell lymphoma. The existing chemotherapeutic agent MMAE is conjugated with an antibody targeted against CD30, which is

upregulated in lymphoma cells. This ADC showed superior efficacy in clinical trials when compared to traditional combination chemotherapy with an objective response rate of 86% versus 30%, respectively. Furthermore, the incidence of myelosuppression was less (14% versus 51%). There are currently four FDA approved ADCs and more in trial ¹⁴.

Nanomedicine

The most recent therapies developed to target malignancies lie at the crossroads where materials engineering and medicine meet. Nanomedicine is defined as the use of synthetic materials between 1 and 100 nm in length to facilitate or enhance the delivery of therapeutic elements. They are composed of a variety of materials, including lipids, carbon, metals, and synthetic polymers. Their small size and biocompatible chemistry allow them to be preferentially absorbed within tumors passively due to a phenomenon known as the enhanced permeability and retention effect (EPR) of cancer. EPR is a function of tumor angiogenesis, in which many new blood vessels are formed throughout the tumor. These blood vessels also exhibit increased “leakiness” as compared to healthy tissue ¹⁵. Furthermore, conjugation with molecules showing preferential uptake by cancer cells allow for nanomaterials to target these cells directly.

Nanomaterials used in medicine are designed to solve two problems. First, they serve to increase the biocompatibility of certain drugs. Amphiphilic lipid-based spheres that are capable of interacting with biological fluids and the membranes of cells can help deliver biocompatible drugs to the targeted cell, for example. Second, they allow for increased cytotoxicity of the payload by shuttling the drugs to cancer cells while shielding the healthy tissue. Their high aspect ratio allows them to carry a large payload that remain inert until they reach the cell. This results in less overall toxicity to the patient. A classic example is Abraxane, a combination of paclitaxel bound to albumin nanoparticles. Abraxane was approved for the treatment of breast cancer in 2005 after clinical studies demonstrated increased tolerance at substantially higher doses than when administered in its traditional form ¹⁶. As of 2017, thirteen anti-cancer nanomedicine therapies were FDA approved with another thirty-six in clinical trials ¹⁷. Below is a summary of the current types of nanomedicine being studied for cancer therapy.

Liposomes

Liposomes were the first nanomaterial drug delivery platform to be approved by the FDA and are the most representative nanomaterial currently on the market¹⁸. Lipid bi-layer spheres form when amphiphilic lipids are added to an aqueous solution that contains the drug. In this way, the drug is incorporated within the sphere. This technology is especially useful for delivering large quantities of water soluble drugs directly to the tumor, avoiding collateral damage to tissue during circulation or rapid clearance through the kidneys¹⁹. Current approved drugs have shown increased delivery to the tumor site and decreased systemic toxicity¹⁶. Liposomal nanoparticles have also successfully incorporated two chemotherapeutic drugs into one platform. For example, Vyxeos is a treatment for acute myelogenous leukemia (AML) which co-encapsulates daunorubicin and cytarabine within a single liposome. The results of the phase III trials demonstrated increased efficacy and decreased toxicity when compared with standard treatment²⁰. This example highlights the feasibility of using a single nanomaterial platform to combine therapies.

Polymeric Nanoparticles

Similar to liposomes, polymeric nanoparticles also create spheres which encapsulate a drug, however they are made out of a variety of synthetic polymers that can be customized to meet specific needs based on the drug being delivered and the target tissue. This platform is especially useful in the delivery of hydrophobic drugs, which can be incorporated into the solvent used during synthesis of the material¹⁵. A prostate cancer therapy is currently available using this platform. Elligard uses the Atrigel® polymer delivery platform in combination with leuprolide acetate which have demonstrated suppressed testosterone concentrations comparable to castration, thus providing a viable alternative to surgery²¹.

Metallic Nanoparticles

Metallic nanoparticles that incorporate metal ions such as gold, silica, silver, and iron are being studied for their use as drug delivery vehicles that also have thermal properties. This allows them to be incorporated into ablation therapies using various forms of heating¹⁶. NanoTherm® uses the injection of iron oxide nanoparticles into glioblastoma tumors followed by the application of MRI. The magnetic

field induces local heating of the nanoparticle, heating the tumor microenvironment to 40-45°C and inducing cell death¹⁶. It was approved by the FDA for the treatment of glioblastoma after clinical trials demonstrated increase in median overall survival of 12 months²². A press release announced in February that MagForce was issued a license to begin clinical trials evaluating this therapy in prostate cancer patients as an alternative to surgery²³.

Carbon Nanotubes

Carbon nanotubes (CNTs) are a nanomaterial with unique physiochemical properties that are currently in the pre-clinical phase of testing as a potential anti-cancer therapeutic. First popularized by Sumio Iijima in 1991, CNTs became an important composite engineering

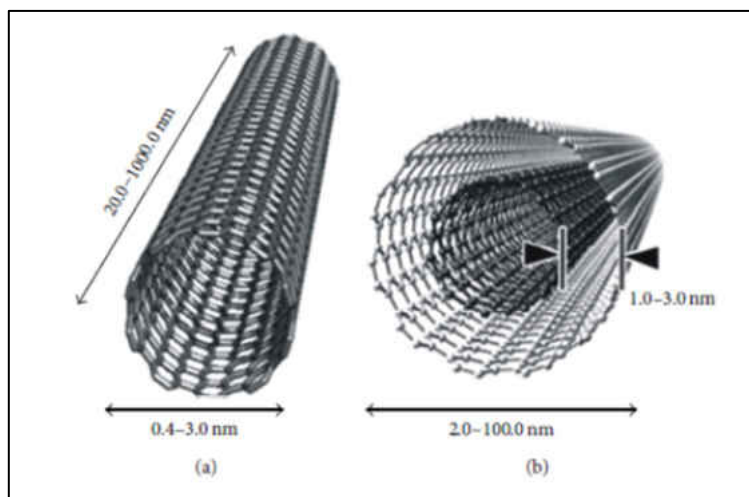


Figure 1. Physical representation of carbon nanotubes. The image illustrates the length and width dimensions. The walls are composed of hexagonal carbon rings in a honeycomb pattern that are rolled into a tube and left singly as a single-walled carbon nanotube (a) or nested as a multi-walled carbon nanotube (b)²⁴.

material due to light weight and tensile strength, which are a direct result of their structure. The material begins as graphite, or sheets of carbon rings arranged in a honeycomb pattern, which is then rolled into a cylindrical shape. These sheets can be assembled as a single layer or nested within multiple layers (Figure 1)²⁴. The hexagonal structure of the carbon coupled with the cylinder shape confers incredible strength to the material. The hollow core within the cylinder makes the material lightweight. However, medicine became interested in CNTs because of their unique physio-chemical properties. First, when the hexagonal carbon rings are arranged in a chiral pattern, they yield semi-metal or semi-conductor properties, which confer optical and thermal properties similar to metallic nanoparticles. This makes them a promising option for hyperthermic ablative therapies²⁴. Second, much like their liposome and polymeric nanoparticle cousins, their surface walls can be modified for the covalent addition of functional groups. This allows for covalent conjugation with other organic compounds, such as cytotoxic

drugs or antibodies. However, CNTs are not naturally amphiphilic like other nanomaterial platforms, but rather are highly hydrophobic in pristine form. This is an undesirable property in the field of nanomedicine where biocompatibility within biological fluids is essential. This challenge can be overcome through functionalization with hydrophilic side groups, making CNTs more dispersible in aqueous solutions^{25 26-28}. Oxidation reactions are one means of covalent functionalization in which oxidizing agents add carboxyl groups to the ends of CNTs and to defects along the wall. Another form of covalent functionalization is achieved through cycloaddition, which adds nitrogen rich groups along sidewalls. Covalent forms of functionalization can be further modified through the addition of polyethylene glycol to increase solubility in biological fluids. While covalent functionalization yields stronger conjugates, the breaking of bonds that exist within the hexagonal carbon rings can weaken the thermal-optical properties intrinsic to CNTs. Non-covalent coating with an amphiphilic molecule which interacts favorably with the hydrophobic surface of CNTs can increase the solubility of the CNT and also serve as scaffolding for conjugation with other compounds, while maintaining the overall optical and semiconductor properties of the material. However, the bond between those molecules is weaker than with covalent functionalization²⁷.

Carbon Nanotube Toxicity:

As the use of CNTs grew in the 1990's, concerns over potential toxicity began to emerge. Early toxicity studies largely centered around the environmental impact of pristine CNTs used in manufacturing which have a fiber-like structure similar to asbestos, a well-known causative agent of mesothelioma. The results of these studies were particularly unfavorable. *In vivo* studies with mice found asbestos-like toxicity when intraperitoneal (IP) injections were administered into abdominal cavities²⁹. Further studies attributed the bio-incompatibility of pristine forms to their high aspect ratios and the hydrophobic nature of the hydrocarbon rings. This leads to a tendency to agglomerate²⁷. Additional *in vivo* studies found that injection with pristine CNTs leads to activation of the innate immune system³⁰, readily initiates the complement cascade³¹ and induces the release of radical oxygen species^{32; 33}.

However, much of these undesirable toxic effects can be overcome through functionalization of the outer walls. Most acute toxicity observed in initial studies was only attributed

nanotubes in pristine form^{29; 30; 32}. As previously discussed, functionalization plays a large role in the biocompatibility of CNTs. Evaluation of functionalized variations of CNTs demonstrate that the mode of exposure, the length of the nanotube and even the number of walls can influence toxicity. Evidence suggests that the number of nested walls could affect cytotoxicity, with multi-walled exhibiting less toxicity than their double and single-walled counterparts^{26; 34}.

Understanding the distribution of CNTs throughout the body and modes of clearance is an important factor when exploring its potential use as a therapy. The route of injection seems to be an important variable. Evidence of deposits have been found in the lungs, liver, spleen, heart, kidneys and lymph nodes following intravenous (IV) injection³⁵⁻⁴³. Whereas subcutaneous (SubQ) injection leads to concentration in the lymph nodes⁴⁴. Interestingly, studies that have used intra-tumor injection have not reported any significant organ biodistribution^{45; 46}.

It is also necessary to explore how CNTs will eventually be cleared from the body. Ideally, a drug should be allowed to remain in circulation long enough to exert the desired therapeutic effect, but also eventually be excreted. It appears that clearance of CNTs is largely related to their the solubility within biological fluids and the ability of the host's immune system to clear the material through the reticular endothelial system (RES)⁴⁷. The RES system consists of mononuclear cells of the innate immune system, primarily macrophages and neutrophils and the organs of the liver, spleen, and lungs. These cells retrieve foreign material or cellular debris via phagocytosis and then channel them primarily back to the liver, where they are eventually cleared through the biliary tract. *In vivo* studies in mice have demonstrated successful clearance of CNTs through RES uptake with varying degrees of efficiency^{42; 48-50}. One factor that effects the rate of clearance is functionalization with polyethylene glycol (PEG). Two separate studies tested different formulations of PEG conjugated to SWCNTs⁴² and MWCNTs⁴⁸ and both concluded that the longer PEG side chains reduced RES clearance. Length also appears to play a role in RES clearance because extremely long CNTs tend to induce frustrated phagocytosis and thereby impede immune cell clearance of the material. Increased length induced frustrated phagocytosis *in vitro* in a macrophage cell

line³⁰, and was also shown to decrease clearance in mice⁴². *In vivo* studies testing radio-labeled CNTs have shown that IV injected CNTs that are hydrophilic can also be cleared through the urinary tract^{49; 50}.

Table 1 summarizes the current body of knowledge surrounding CNT biodistribution, clearance, and immune activation based on route of injection and CNT composition. The varying results seen in the degree of toxicity noted and biodistribution between studies can be largely attributed to the wide range in length, number of walls and modes of functionalization of the CNTs employed in these experiments. This makes direct comparisons between constructs difficult and highlights the importance of exploring biodistribution and toxicity with any novel system being evaluated.

Table 1. Biodistribution of CNTs.

Route of Injection	Type of CNT	Organ system
<i>Biodistribution</i>		
IV	purified SWCNT with Tween®	liver, lung, and spleen ³⁵
IV	DTPA- and NH ₃ -MWCNTs	liver and lung ³⁶
IV	PEGylated-SWCNT	liver and splenic macrophages ³⁷
IV	MWCNT	heart, lung, spleen, and kidney ³⁹
IV	HCPT-MWCNT*	liver, spleen, lung and kidney ³⁸
IV	CAHA-SWCNT-Dox**	liver and spleen ⁴⁰
IV	HA-MWCNT-Dox	liver, spleen, and lungs ⁴¹
IV	PEGylated SWCNT-RGD***	liver and spleen ⁴²
IV	DOTA-SWCNT-Rituximab	kidney, liver, spleen, and bone ⁴³
SubQ	MWCNTs	Lymph nodes ⁴⁴
Intra-tumor	MWCNT suspended in Pluronic F127	No evidence ⁴⁵
Intra-tumor	NH ₃ -MWCNT-siRNA	No evidence ⁴⁶
<i>Clearance</i>		
IV	PEGylated SWCNT	RES uptake ⁴²
IV	hydroxyl-PEGylated MWCNT	RES uptake ⁴⁸
IV	DTPA-MWCNT	kidney and biliary Tract ⁴⁹
IV	dye-conjugated SWCNT	Intestines ⁵¹
IP	MWCNT	kidney and biliary Tract ⁵⁰
<i>Immune Response</i>		
SubQ	oxidized MWCNT	macrophage phagocytosis, complement activation ³³
IP	pristine MWCNT	frustrated phagocytosis, granulomas ²⁹
macrophage cell culture	pristine MWCNT	frustrated phagocytosis ^{30; 32}

* HCPT: 10-hydroxycamptothecin

** CAHA: cholanic acid-derivatized hyaluronic acid; DOX: doxorubicin

*** RGD: arginine-glycine-aspartic acid

Carbon Nanotube Conjugates:

Another benefit of functionalization is that it provides chemical side groups that can bind other molecules. Conjugation with a number of molecules to enhance cancer cell uptake have been explored which increase tumor absorption both passively and directly. Suspension in biological surfactants^{45; 52} and nucleic acids^{53; 54} increase CNT dispersion, and allow the tiny materials to exploit the EPR seen in many cancers, allowing for increased passive uptake into cancer cells. Targeted uptake has been achieved through conjugation with monoclonal antibodies. Further conjugation with existing cytotoxic drugs, such as doxorubicin^{41; 55; 56}, 10-hydroxycamptothecin³⁸, and interfering nucleotides^{28; 46} have demonstrated enhanced cytotoxicity to the malignant cells while showing decreased toxicity to healthy cells.

Carbon nanotubes as Electric-thermal Conductors:

CNTs also exhibit useful photo-thermal properties which can be exploited to detect and treat cancer. Semi-conducting SWCNTs exhibit photoluminescence in the near infrared region (NIR) of the light spectrum, with an emission range of 800-2000 nm, well within the biological transparency window⁵⁷. Because of this property, SWCNTs have been successfully used as biosensors and optical probes⁵⁸⁻⁶⁰. Conversely, MWCNTs possess electrical antenna properties that allow for the absorbance of approximately three times the amount of light as SWCNTs, generating heat with a high degree of efficiency⁵². Intra-tumor injections with SWCNTs in combination with NIR laser irradiation have demonstrated selective ablation of tumor cells with minimal damage to healthy tissue and increased host survival^{45; 53}. Another study coupled an infrared fluorescent cyanin with a PEGylated SWCNT to complete image guided ablation via intravenous injection and NIR⁵¹. Jeyamohan et al. demonstrated the usefulness of CNTs as a platform for combination therapy by conjugating CNTs with the chemotherapeutic doxorubicin and then applying NIR, where they achieved 95% tumor cytotoxicity *in vitro*⁶¹.

Carbon Nanotubes and Microwaves:

NIR only allows gradual, non-uniform heating of cells which necessitates a lengthy irradiation time even with the acceleration of hyperthermia facilitated by CNTs. Electromagnetic microwaves on the other hand, rapidly generate heat within CNTs through the Joule effect. This form of

heating, which transfers the kinetic energy of excited molecules into heat through friction, exhibits superior penetration depth and lower absorbance by biological tissues as opposed to NIR. One promising physical characteristic of MWCNTs, is that relatively low levels of microwave energy are capable of causing CNTs to reach temperatures capable of causing cell ablation⁶². In fact, application of microwaves to dry CNTs have demonstrated heating rates of 236 °C/min and temperatures as high as 1000 °C⁶³. Earlier experiments performed by this lab were the first to evaluate microwave-induced hyperthermia *in vitro* and *in vivo*. In these studies, researchers demonstrated selective cytotoxicity to cancer cells through treatment of antibody-conjugated carbon nanotubes in combination with microwave irradiation⁶².

Combination Therapies

Combining these different approaches to treating cancer has become the cornerstone of modern oncology and led to the concept of a cure. In the 1960s when physician scientists began combining aggressive treatment regimens of four different chemotherapeutic agents for childhood acute lymphoblastic leukemia (ALL) and Hodgkin's lymphoma, the remission rate for ALL rose from 25% to 60% and the complete remission rate rose from nearly zero to 80% for Hodgkin's lymphoma. Similar treatment schedules are still in place today for these cancers⁴. Once researchers established that cytotoxic therapies could successfully cause remission and even cures in patients, they began investigating approaches that would target the cancers more effectively and decrease toxicity. One approach is to use a combination of different anti-cancer modalities such as surgery, laser treatment, radiation and chemotherapy. This allows a decrease in the dose of individual cytotoxic drugs, and has resulted in less overall incidence of adverse effects in patients. Furthermore, attacking cancer cells from many different angles may help decrease drug resistance due to the heterogeneity of tumors. Innovations in materials and immuno-engineering have allowed unique opportunities to address many of the challenges in making cancer therapy targeted to the malignant cells. Incorporating these newer methods along with traditional approaches are a promising new direction in increasing survival rates of cancer patients.

III. Purpose of this Study

The purpose of this study is to continue to evaluate the effects of ab-MWCNTs in combination with microwave irradiation as a potential anti-cancer ablation therapy. This construct is being evaluated as a potential tool to combat prostate cancer. Prostate cancer is the leading cause of cancer and the second leading cause of cancer deaths in males in the U.S. ¹ Surgery for prostate cancer can be curative, but metastatic cancer requires a combination of hormone therapy, chemotherapy, immunotherapy, and/or irradiation ⁶⁴. This proposed treatment could be incorporated into a combination therapy alongside those currently approved to improve outcomes in these patients. The proposed treatment involves intra-tumor injection with ab-MWCNTs conjugated with an antibody specific to an antigen overexpressed on prostate cancer cells. This confers specificity and targets the nanomaterial to the tumor and away from healthy tissue. Following the injection, low levels of microwave irradiation are administered. The physio-chemical nature of CNTs described above allows this material to reach cell-death inducing temperatures at levels low enough to avoid damage to healthy cells.

Previous work performed by Beckler et al. first demonstrated proof of concept for this treatment. *In vitro* cell culture studies were performed in which PC3 prostate cancer cells were treated with varying concentrations of ab-MWCNTs conjugated with anti-CD44, an antibody targeting a protein that is highly expressed on prostate cancer cells, and then exposed to varying settings of microwave irradiation. Several key discoveries were made from this seminal work. Most notably, researchers proved for the first time that ab-MWCNTs in combination with microwave irradiation exert significant cell death in PC3 tumor cells when compared to HPEC control cells (61% vs. 22%), highlighting the critical role that antibody-conjugation plays in delivery of hyperthermic agents. Second, these studies showed that concentrations of ab-MWCNTs exceeding 0.25 mg/mL induce cell death to the PC3 and control cells even without microwave irradiation in cell culture. This suggests that high concentrations of ab-MWCNTs alone may play a role in inducing cell death. Furthermore, they established that concentrations of at least 0.1 mg/mL of MWCNTs are necessary to exert a significant hyperthermic affect when combined with microwave irradiation. These two concentrations suggest a therapeutic window of 0.1 mg/mL to 0.25 mg/mL as optimal

when designing future studies. Finally, experiments that optimized the microwave settings found that shorter bursts of higher wattages (900W for 7 seconds) were tolerated by both PC3 cells and HPEC cells when compared to equal energy dispersed as lower wattages over a longer period of time (40W for 205 seconds). While both of these settings administer roughly the same overall amount of energy, 6300 and 8200 Joules (J) respectively, the delivery of this energy can have implications on the cellular level and are therefore an important factor when considering collateral damage to surrounding healthy tissue⁶³.

These researchers also demonstrated efficacy *in vivo* using live zebrafish-PC3 xenograft embryos. In these experiments, PC3 cells previously treated with 0.1 mg/mL ab-MWCNTs were injected into the zebrafish embryos. These embryos, along with control groups were then subjected to 900W of microwave for 7 seconds. The results revealed that only the xenograft embryos that received treated cells showed significant cell death following microwave irradiation, whereas zebrafish xenograft embryos that were not treated with ab-MWCNTs exhibited virtually no cell death. Furthermore, the embryos were unharmed and continued to develop normally. This proved that the combination therapy demonstrated in cell culture was feasible in a living model⁶³.

The physiology between zebrafish embryos and humans is obviously quite different, therefore the next step is to show that hyperthermic ablation can be achieved in a higher mammalian model. The overarching goal of this project is to continue evaluating the proposed treatment in mice. The antibody that is conjugated to the MWCNTs in this study is targeted against the prostate specific membrane antigen (PSMA). This is a transmembrane protein that is found in low levels on normal prostate cells, but is highly upregulated in tumor cells, and expression increases with severity of clinical disease⁶⁴. The previous work described by Beckler et al. used an antibody against CD44, which is a cell surface marker found to be upregulated in cancer stem cells. Cancer stem cells are often difficult to kill and are thought to be a leading cause of tumor drug-resistance, making them an ideal target for precision therapies. However, CD44 is expressed on a variety of other healthy tissues as well and has demonstrated toxicity related to its cross reactivity with those tissues⁶⁵. It is important to note that isotopes of PSMA have also been found in other tissues. Histochemical staining has shown the protein to be present in the renal tubules, the brush lining of

the jejunum and in nervous system glia⁶⁶, however prostate tumor expression levels are 1000-fold greater than the minimal expression patterns seen in these tissue⁶⁷. While concern for causing collateral damage to healthy tissues expressing PSMA is valid, the clinical trials using anti-PSMA to deliver radioisotopes and cytotoxic drugs are underway and demonstrated toxicity attributed to the payload rather than cross-reactivity⁶⁸. For these reasons, monoclonal anti-PSMA is a superior antibody in which to target prostate cancer cells.

In continuation of the previously described work, this study tested three hypotheses. The first hypothesis is that injected antibody-conjugated MWCNTs (ab-MWCNT) followed by microwave irradiation can cause hyperthermic ablation in mice. Successful ablation of tumor cells in zebrafish embryos have already been demonstrated. Before testing efficacy in a tumor model, it is prudent to attempt a proof of concept in a healthy mouse model. No one has ever published a study examining these effects in mice. It is unclear whether mice will even tolerate the proposed treatment. For that reason, this hypothesis is tested in normal healthy mice via IM injection and evaluation of muscle cell necrosis is evaluated. It is predicted that histological examination of the muscle at the site of injection will demonstrate cell death in the form of necrotic ablation of the muscle. Should the hypothesis be accepted, this will lend support for testing this regimen for efficacy as an anti-cancer therapy in a tumor mouse model.

The second hypothesis is that the injected ab-MWCNTs will remain localized at the site of injection. This is evaluated through histological examinations of tissue over time. It is predicted that the ab-MWCNTs will be present in muscles sectioned at 24 hours, 1 week, and 2 weeks post injection. Sections of the vital organs processed at the same time points are not expected to demonstrate evidence of ab-MWCNT migration. This is largely expected based on review of the literature. There are no studies that have examined IM injections of CNTs. The most similar route of administration is intra-tumor and those studies have not shown evidence of significant biodistribution to other organs.

The third hypothesis is that the innate immune system will mount an inflammatory response to the injection of ab-MWCNTs. Previous studies have demonstrated that the phagocytic white blood cells (WBC) of the innate immune system, namely neutrophils and macrophages, recognize CNTs as

a foreign substance³². Incorporating a monoclonal antibody to the surface of the MWCNTS can enhance this effect, especially if areas of the Fc portion are not anchored within the complex. Macrophages and neutrophils have receptors that specifically recognize this region of antibodies as part of the fundamental process whereby antibodies coat, or opsonize, foreign materials for recognition and clearance by the phagocytic cells of the innate immune system⁶⁹. While it is desirable for the ab-MWCNTs to eventually be cleared through the RES system, rapid clearance before application of the microwave would impact the effectiveness of the proposed treatment. Comparing the level of inflammation between the groups that are injected with ab-MWCNTs and those that receive plain MWCNTs may serve as a quality indicator for the antibody conjugation method employed during synthesis. Given the previous studies that have demonstrated RES clearance of a variety of CNTs, it is expected that neutrophilic infiltration of the muscle at the site of injection will occur to some degree in groups that receive both the ab- and plain MWCNTs. If extensive ablation occurs as a result of microwaved induced hyperthermia of the MWCNTs, it is expected that treatment groups which receive the combination therapy will demonstrate increased infiltration, as these cells attempt to also clear the debris from the necrotic muscle cells.

Finally, this study will further analyze the neutrophil and macrophage response to ab-MWCNT using transgenic zebrafish embryo models that express green fluorescent proteins (GFP) in neutrophils and macrophages. These embryos will be injected with ab-MWCNTs that incorporate a fluorochrome and the WBC response will be evaluated using fluorescent confocal microscopy with time-lapse software. This type of imaging allows evaluation of these cells' interaction with the injected ab-MWCNTs in real-time. It is predicted that they will infiltrate the areas of the embryos that are concentrated with ab-MWCNTs and that they will attempt to clear the ab-MWCNTs via phagocytosis.

CHAPTER 2

MATERIALS AND METHODS

I. Preparation of Antibody-Conjugated MWCNTs

Dr. Quirino's lab in the Chemistry Department at Georgia Southern University (Statesboro, GA) prepared the carbon nanotubes used in the experiments. Figure 2 provides a schematic for the chemical modifications made during preparation⁶³. MWCNTs were purchased from Cheaptubes (Grafton, VT) and oxidized with a 2 hour incubation in an ozonator. This step further served to sterilize the MWCNTs. The oxidized MWCNTs were then sonicated, followed by the addition of sterile NHS, EDAC, and 0.5M MES buffer. The mixture was spun on a hot plate for one hour, vacuum filtered, and then placed in a 70° C vacuum oven overnight to dry. This process creates the functional groups necessary to form a peptide bond with the N-terminus regions of the antibody. The esterified-MWCNTs were then sonicated with 0.5M MES buffer. The antibody was added to the solution and allowed to stir with a siliconized stir-bar on a hot plate for 1 hour. The solution was centrifuged for 5 minutes at 5000 rpm. 0.5M MES buffer was added to reach the appropriate concentration. Antibody conjugation was verified through fluorescent microscopy. Anti-PSMA AlexaFluor488® (BioLegend, San Diego CA) was used for the mouse studies. This is a murine IgG antibody that emits green fluorescence when excited by 488nm wavelengths of light. Its specificity is to human PSMA. This specificity was chosen because future experiments will include mice with human prostate tumor xenografts. Anti-PSMA AlexaFluor488® could not be used for the zebrafish embryo studies because it fluoresces at the same wavelength as the GFP that are expressed by the cells of interest in the embryos. In order to contrast, an antibody was chosen that fluoresces red when excited by 647nm wavelengths of light. Anti-human AlexaFluor647® (BioLegend, San Diego CA) was used for these studies. This is also a murine IgG antibody with specificity to human cells.

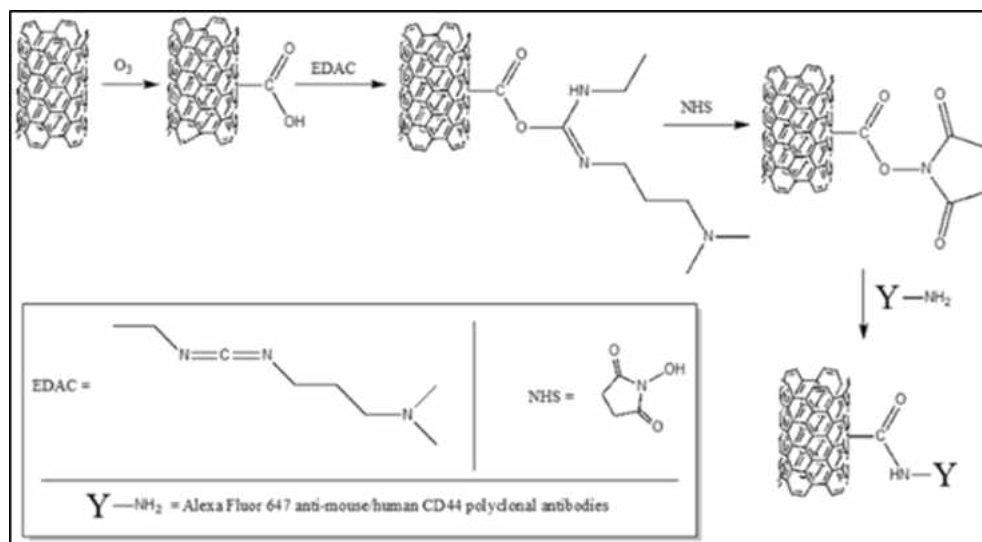


Figure 2. Preparation of antibody-conjugated MWCNTs. Illustrations of the chemical functionalization of the MWCNTs and the conjugation of an antibody⁶³.

II. Microwave Irradiation Optimization

As part of the experiment, mice were anesthetized and treated with full body microwave irradiation with the Milestone Ethos Synth 1600 URM microwave labstation (Soriso, Italy). This source delivers 2450 MHz microwaves at powers and durations selected by the user. A microwave optimization schedule was developed to find the highest tolerable dose for the mouse model. Establishing an optimal irradiation schedule must take into account the total energy delivered, as well as the power and duration by



Figure 3. Milestone Ethos Synth 1600 URM Microwave Labstation with control unit.

which it is delivered. Total microwave energy is calculated using the following formula:

$$\text{Energy (Joules)} = \text{Power (Watts)} \times \text{Time (sec)}$$

The original design was based on results obtained from the previously described *in vitro* and *in vivo* studies that determined that shorter bursts of higher wattages were best tolerated⁶³. The optimum schedule in these studies was 6300 J delivered as 900 W for 7 seconds. The concern was that the physiology of the mice would make it more difficult for the microwaves to penetrate the tissue and it was believed that this amount of irradiation would not be sufficient. The initial design was to treat 2 mice to each of the following settings: 900 W for 7 seconds (6300 J), 10 seconds (9000 J), and 15 seconds (13,500 J). The lowest proposed setting was lethal to the first mouse, so the design was revised. Two mice were treated with 100W for 5 seconds (500 J), one mouse with 150 W for 5 seconds (750 J), 1 mouse with 200W for 5 seconds (1000 J), and 1 mouse with 450 W for 3 seconds (1350 J). They were monitored for 48 hours for tolerance. Tolerance was determined based on emergence of symptoms within 48 hours post treatment. Symptoms are defined as fatality, elevated respiration rate, visible lesions and burns or abnormal behavior. The highest dose tolerated was chosen for the experiments.

Table 2. Microwave optimization schedule.

Wattage and Duration	Total Energy (Joules)
100 W for 5 seconds	500 J
150 W for 5 seconds	750 J
200 W for 5 seconds	1000 J
450 W for 3 seconds	1350 J
900 W for 7 seconds	6300 J

III. Mice

All research was conducted at Georgia Southern University in Statesboro Georgia in accordance with Institutional Animal Care and Use Committee approval. 4-5 week old male C57BL/6 mice were acquired from Jackson Lab (Bar Harbor, ME) and housed at the Georgia Southern University fieldhouse (Statesboro, GA). C57BL/6 mice are an inbred strain originally developed by Jackson Labs in the 1920's for cancer and immunology studies⁷⁰. This strain of mice is the most widely used model for

toxicology studies, cited by more than 25,000 papers. They were chosen for this study because of their reliable track record as a dependable model with a generic genetic background and robust innate immune system⁷¹. Upon receipt, they were given a unique ear punch identifier, weighed, and randomly assigned to an experimental group. Mice were kept 3/cage, had free choice of food and water, and were maintained on a 12 hour light/dark schedule. Cages were monitored daily for food and water and cleaned at least twice per week.

IV. Mice Experimental and Control Groups

Mice were assigned to three large groups based on the length of time they would be monitored post treatment before necropsy: 24 hours, 1 week, and 2 weeks. These groups were further stratified into subgroups that would serve as controls and the treatments which isolate three variables of interest: antibody, MWCNT concentration, and microwave. The lowest concentration chosen was based on *in vitro* studies previously described which indicated that concentrations between 0.1 and 0.25 mg/mL were optimal for causing hyperthermic cell death without toxicity from the MWCNTs themselves⁶³. The higher concentration chosen was 0.5 mg/mL. This is outside of the window established by the cell culture studies, however the route of injection limits the total volume administered to 0.02 mL. Therefore, mice in these groups would only be receiving a total of 10 µg of MWCNTs, comparable to other cited studies where the total administration of CNTs via intra-tumor injection was between 10-100 µg^{45; 46}. Note that an injection only control group was not chosen because studies have shown that injection of sterile solutions alone does not cause a localized immune response⁷². Additional costs did not outweigh the benefits of adding more mice. Table 3 outlines these subgroups: A) No treatment, B) Microwave only, C) 0.125 mg/mL ab-MWCNT only, D) 0.125 mg/mL plain MWCNT PLUS microwave, E) 0.125 mg/mL ab-MWCNT PLUS microwave, F) 0.5 mg/mL ab-MWCNT only, G) 0.5 mg/mL plain MWCNT PLUS microwave, H) 0.5 mg/mL ab-MWCNT PLUS microwave.

Table 3. Mice experimental and control groups.

Group	MWCNT Concentration (mg/mL)	Antibody Conjugation	Microwave Irradiation
A			
B			yes
C	0.125	yes	
D	0.125		yes
E	0.125	yes	yes
F	0.5	yes	
G	0.5		yes
H	0.5	yes	yes

V. Anesthesia

Prior to treatment, animals were anesthetized using a ketamine (80 mg/kg)/xylazine (10 mg/kg) (MWI Animal Health, Boise ID) cocktail which was mixed in-house. The solution was prepared by adding 0.2 mL ketamine (100mg/mL), 0.1 mL xylazine (20mg/mL), and 3.7 mL of sterile DI water to a sterile red top vacutainer tube. The solution was discarded after immediate use. Each mouse received 0.02 mL/gram body weight via intraperitoneal injection (IP). The average 20 gram mouse received 0.4 mL and achieved a 40-50 minute sedation. Mice were tested for reflex using a toe pinch procedure to ensure sedation was achieved. Mice were continuously monitored post procedure for 2 hours to ensure that they were fully awake and capacitated. The site of injection was cleaned with 70% ethanol and each mouse received a fresh sterile syringe and needle.

VI. Injection of MWCNTs

After ensuring sedation was achieved, mice in the respective treatment groups received 0.02 mL IM injections to the right caudal thigh muscle of 0.125 mg/mL or 0.5 mg/mL ab-MWCNTs or plain MWCNTs (Figure 4)⁷³. The solutions were vortexed before each syringe was prepared. The site of injection was cleaned with 70% ethanol and each mouse received a fresh sterile needle and syringe.

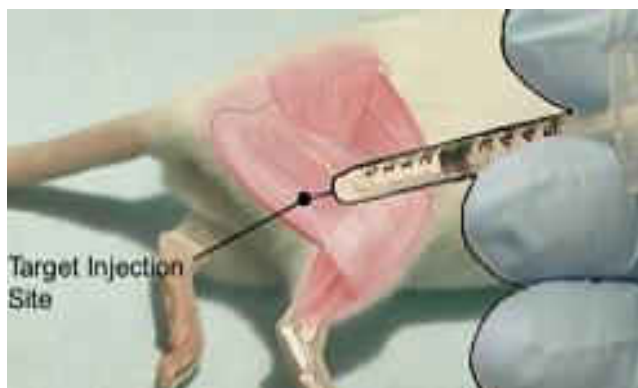


Figure 4. Demonstration of intramuscular injection⁷³.

VII. Microwave Irradiation

Mice in the experimental groups that were to receive microwave irradiation were placed into the chamber on a Teflon surface in the prone position with their tails wrapped to the right to expose the right rear flank where the injections occurred. They were treated with a constant source of 150W microwave irradiation for 5 seconds. The plate spun at a constant rate to evenly distribute the rays. The period between MWCNT injection and microwave irradiation was 30-45 minutes. Mice were returned to their cages and monitored for any adverse events.

VIII. Euthanasia

Mice were euthanized using a compressed CO₂ gas chamber with a flow rate which displaced 10-30% of the air with CO₂. Euthanasia was verified by decapitation using a guillotine. Blood was collected via the trunk for serum studies performed by a collaborating lab. Mice underwent a full necropsy. The injected muscle, brain, heart, lungs, liver, spleen, kidneys, and testes were placed in 10% neutral buffered formalin (Fisher Scientific, Hampton NH). Portions of the heart, liver and kidney were also frozen via liquid nitrogen bath for RNA expression analysis.

IX. Tissue Preparation

After fixing for at least 48 hours in formalin, organs from 3-4 mice per experimental group were packaged into histology cassettes (Fisher Scientific, Hampton NH). The heart, lungs, brain, and testes went into one cassette; the liver, spleen, and kidney went into another; and the injected leg went into a final cassette. The tissue was sent to University of Georgia Veterinary Pathological Services (Athens, GA) for paraffin embedding and tissue sectioning. Tissue was sectioned at a depth of 30 μm into sections 4 μm thick. The slides were then stained with Hematoxylin and Eosin (H&E), permanently cover-slipped and returned to Georgia Southern University (Statesboro, GA).

X. Slide Analysis

All slides were examined under brightfield microscopy at 100x, 200x, and 400x total magnification. Evidence of MWCNTs, hyperthermic necrosis and neutrophil infiltration were evaluated at the site of the injection in the muscle. In muscles where the site of the injection was not evident, deeper cuts were made and slides prepared as described previously. The organs were scanned for evidence of morphological changes due to hyperthermic necrosis or inflammation and MWCNT presence. Necrosis and inflammation was graded as present or absent

XI. Zebrafish Embryo

Zebrafish have become a favorable choice for *in vivo* imaging studies due to their translucent physiology, existence of many transgenic lines that express green fluorescent proteins in specific cells, and the fact that the genome remains largely conserved compared with humans⁶². Two transgenic lines of Zebrafish (*Danio rerio*) were acquired. The *Tg(mpeg1::gfp)* fish express green fluorescent protein (GFP) in the macrophages and *Tg(mpx1::gfp)* fish express GFP in the neutrophils. Embryos were harvested and immediately treated with 50 μL 1-phenyl 2-thiourea (PTU), a chemical which suppresses pigment production and yields clearer images. Zebrafish were maintained in a laboratory

breeding colony in the Georgia Southern University fieldhouse. Fish were kept on a 14/10h light/dark cycle. Embryos were incubated at 28.5°C.

XII. Confocal Fluorescent Microscopy and Time-Lapse Imaging

48 hours post-fertilization, zebrafish embryos from both transgenic lines were injected with 1-2 μ L of undiluted MWCNTs conjugated with anti-human AlexaFluor647®. Embryos were anesthetized with tricain and mounted in 5% low melting agarose then flooded with embryo medium into 4x4 wells. The entire embryo was examined under fluorescent microscopy. All time-lapse videos were performed on a Carl Zeiss LSM 710 confocal fluorescent microscope and processed using ZEN 2.1 SP3 FP3 software.

Studies to examine neutrophil interaction with ab-MWCNTs were performed using 8 *Tg(mpx1::gfp)* embryos under 100x total magnification. Embryos were mounted immediately following injection. Z-stack depth was obtained based on the depth the fluorescence was presenting. Imaging was programmed to take Z-stack images every 10 minutes for 2 hours. Images on the remaining 4 embryos were then obtained at 24 hours post injection and again on the 2 remaining embryos 72 hour post injection.

Studies to examine the macrophage interaction with ab-MWCNTs were performed using 4 *Tg(mpeg1::gfp)* embryos mounted in the same manner. Imaging was programmed to take Z stack images every 3 minutes for 2 hours at 200x total magnification on embryos immediately following injection. The remaining embryo was imaged again after 24 hours post injection.

XIII. Statistical Analysis

The frequency of hyperthermic necrosis at the site of injection in the mice studies was evaluated using the χ^2 frequency distribution analysis in using JMP® software to determine significant differences between treatment groups. Inflammation at the site of injection and other morphological changes in organ tissue was evaluated qualitatively. Zebrafish embryo experiments were also evaluated qualitatively.

CHAPTER 3

RESULTS AND DISCUSSION

I. Antibodies are Effectively Conjugated to MWCNTs

The antibody attached to the outer walls of the MWCNTs is what allows the compound to target cancer cells. Antibody conjugation is an essential part of the proposed treatment that will be tested in future prostate cancer xenograft mice. In order to verify the conjugation was successful, a sample from each batch was observed under fluorescent microscopy before injection. Fluorescence was observed on the surface of undiluted

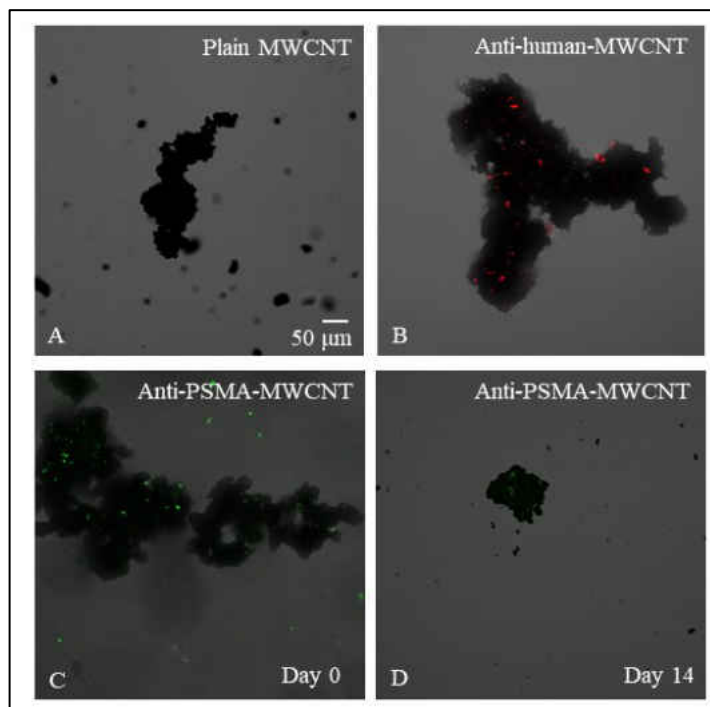


Figure 5. Analysis of antibody conjugation. Images compare plain MWCNT without antibodies (A) as compared with MWCNTs conjugated with anti-human AlexaFluor647® (B) and anti-PSMA AlexaFluor488® on the first day of synthesis (C) and on day 14 (D). 400X Total Magnification.

MWCNTs conjugated with anti-human Alexafluor647® (Figure 2-A) and anti-PSMA Alexafluor488® (Figure 2-B) on the first day of synthesis and up until day 14 (Figure 2-C and D). This verifies that the covalent bond between the MWCNTs and the antibodies is stable for at least 2 weeks *in vitro*. This is a sufficient time window because all of the experiments testing this construct were performed within the two week timeframe. The integrity of the ab-MWCNTs may in fact be much longer, as the decrease in fluorescence may be a function of decay of the dye rather than an indicator of dissociation of the antibody. Biologically, it is only important that the antibody remain conjugated long enough to reach its target. However, knowing the half-life of the conjugation would help with the logistics of orchestrating the many components that are involved in these types of experiments. Future studies may look at a more

quantitative way to measure the decay of antibody fluorescence over this time span. This is a challenge because it is impossible to view the same particle during each daily measurement. However, taking an average of multiple samples daily may provide a statistical way to overcome this barrier

II. Microwave Irradiation Optimization

Mice were evaluated for tolerance of various levels of total microwave energy as expressed in Joules. The 4500J (900W for 5 sec) and 1000J (200W for 5 sec) trials were fatal. The 1350J (450W for 3 sec) trial was not fatal, but the mouse experienced elevated respiratory rate, increased body temperature and surface burns on the tail and the exposed right hind foot. The 750J (150W for 5 sec) and 500J (100 W for 5 sec) trials were tolerated

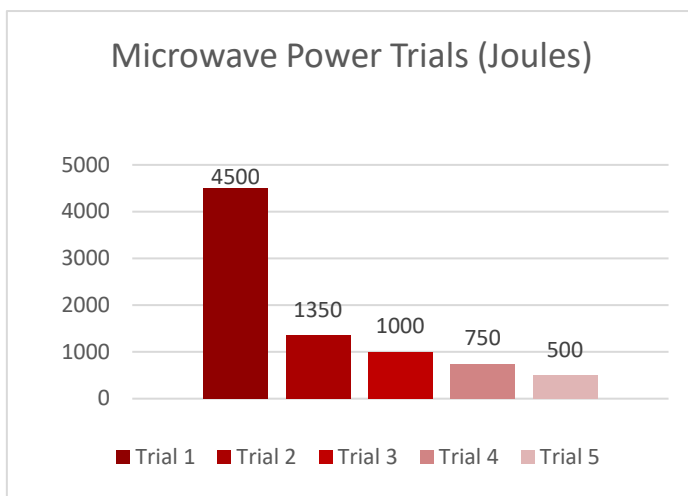


Figure 6. Power optimization trials. Individual microwave trials to determine the optimal dose for mice experiments. The trials pictured in red (1, 2, and 3) indicate total microwave energy that was not tolerated. Those expressed in pink indicate tolerated doses (4 and 5).

well by the mice, therefore the highest energy of 750J was chosen as optimal for the subsequent experiments (Figure 6). The results of the trial are somewhat surprising given that studies evaluating this construct in zebrafish showed viability of the embryos with up to 9000J of energy⁶³. It is likely that the aqueous medium they were suspended in acted to absorb a portion of the microwaves and served as a buffer.

III. Necrosis was Observed at the Site of MWCNT Injection

H&E stained sections of the injected caudal thigh muscle were scanned for evidence of MWCNTs (Figure 7). The MWCNTs were clearly visible as dark, non-refractile carbon clumps (Figure 7, red arrows). Once the site was detected, deviations from normal muscle morphology were observed. Hyperthermal necrotic muscle cells are characterized by loss of clear cell membrane, deterioration of muscle fibers and pallor as compared with healthy cells (Figure 7 black arrows). Neutrophils were also observed infiltrating

the muscle and surrounding the MWCNTs. These cells are characterized by their deep purple staining clefted or kidney bean shaped nucleus (Fig. 7-A). This is another indication of cell necrosis as well as a sign of a primary immune response. Other immune cells were observed, such as eosinophils and macrophages, however the neutrophils predominate. These different changes in morphology are further discussed below.

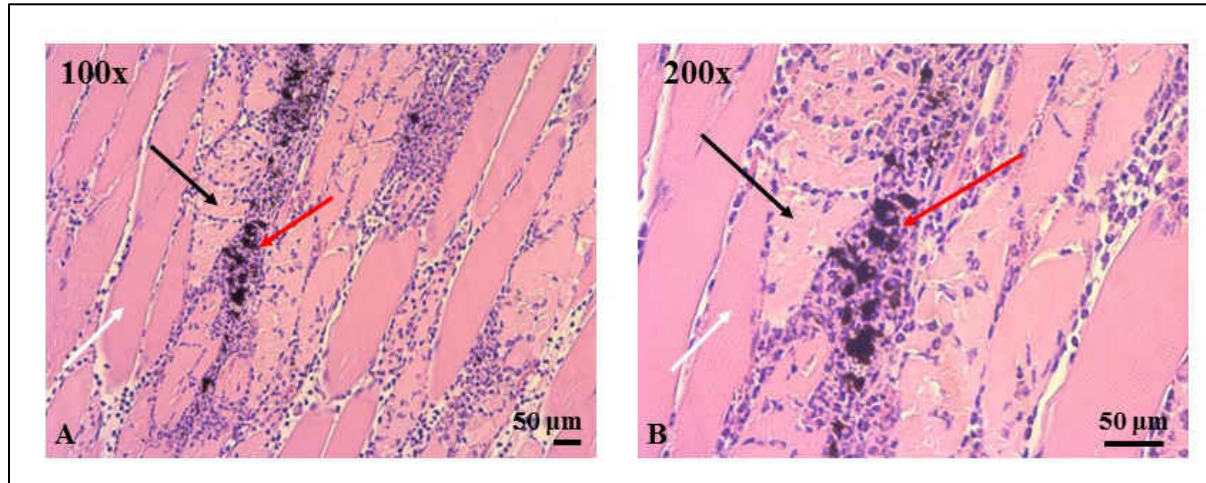


Figure 7. Histology demonstrating types of necrosis. H&E stained tissue section of muscle demonstrating a lesion found at the site of MWCNT injection at multiple powers. A) 100x total magnification demonstrates the width of the lesion compared to normal healthy muscle. B) 200X total magnification allows better visualization of MWCNTs surrounded by neutrophils (red arrow) and a necrotic cell characteristic of hyperthermic ablation (black arrow).

MWCNTs plus Microwave Induces Hyperthermic Necrosis

Slides were evaluated for the presence or absence of hyperthermic necrosis and compiled into frequency distribution tables based on experimental groups. Differences in frequency distributions between groups necropsied at each given time-point (i.e. 24 hours, 1 week, and 2 weeks post treatment) were compared with one another using χ^2 analysis (Table 4A-C, respectively) and evaluated for statistical significance ($p < 0.05$). Because any hyperthermic necrosis that occurred did so at the time of microwave treatment, individuals from each of the three time points were combined into the stratified experimental groups to increase statistical power (Table 4D).

Table 7-D. χ^2 values comparing hyperthermic necrosis frequencies between groups sacrificed at all time-points combined. Values in bold represent a statistically significant difference between the frequency distributions of the two compared groups ($p < 0.05$). All comparisons that yield a result share 1 degree of freedom. The χ^2 values of 0 indicate identical frequency distributions.

	All Groups						
	(B) Microwave Only	(C) 0.125 mg/mL ab-MWCNT	(D) 0.125 mg/mL MWCNT + microwave	(E) 0.125 mg/mL ab-MWCNT + microwave	(F) 0.5 mg/mL ab-MWCNT	(G) 0.5 mg/mL MWCNT + microwave	(H) 0.5 mg/mL ab-MWCNT + microwave
(A) No treatment	0	0	6.097	11.457	0	9.276	11.457
(B) Microwave Only	-	0	6.097	11.457	0	9.276	11.457
(C) 0.125 mg/mL ab-MWCNT	-	-	6.097	11.457	0	9.276	11.457
(D) 0.125 mg/mL MWCNT + microwave	-	-	-	1.369	6.556	0.446	1.369
(E) 0.125 mg/mL ab-MWCNT + microwave	-	-	-	-	12.242	0.305	0
(F) 0.5 mg/mL ab-MWCNT	-	-	-	-	-	9.969	12.242
(G) 0.5 mg/mL MWCNT + microwave	-	-	-	-	-	-	0.305

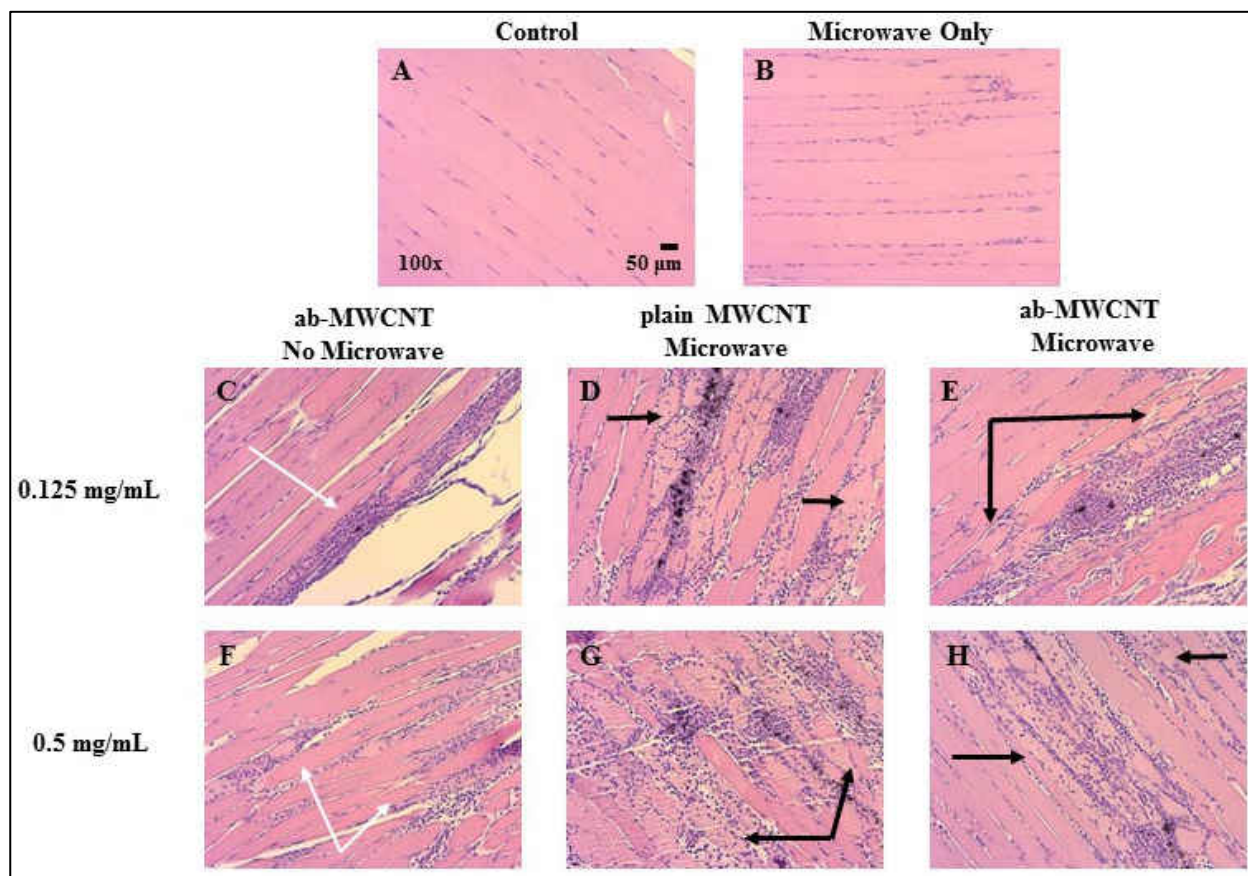


Figure 8. Histology demonstrating necrosis in treatment groups. H&E tissue slices of muscle from mice sacrificed 24 hours post treatment. Hyperthermic necrosis of the CNT plus microwave groups (black arrows: D, E, G, and H) is demonstrated as compared to the purely inflammatory necrosis in the groups that received no microwave (white arrows: C and F) and the controls (A and B). [A: no treatment, B: Microwave Only, C: 0.125 mg/mL CNT plus antibody, D: 0.125 mg/mL CNT plus microwave, E: 0.125 mg/mL CNT plus antibody plus microwave,

There was no incidence of hyperthermic necrosis in any of the slides from mice that received only MWCNTs without microwave (Figure 8D and F) or microwave alone (Figure 8B). Necrosis to muscle cells surrounding the MWCNTs was only seen in slides from mice that received both MWCNT injections in combination with microwave irradiation (Figure 8D, E, G, and H). Comparisons of frequency distributions reveal a statistically significant increase in necrosis for all treatment groups that received this combination (Groups D, E, G, and H) when compared to the control (Table 4. $\chi^2 = 6.097$, $df = 1$, $p = 0.0135$; $\chi^2 = 11.457$, $df = 1$, $p = 0.0007$; $\chi^2 = 9.276$, $df = 1$, $p = 0.0023$; $\chi^2 = 11.457$, $df = 1$, $p = 0.0007$, respectively). Comparisons between groups that received ab-MWCNT and microwave (E and H) to the group that received only ab-MWCNTs without microwave (C and F) for their respective concentrations yield similar results as when compared to the controls (Table 4. $\chi^2 = 11.457$, $df = 1$, $p = 0.0007$ and $\chi^2 = 12.242$, $df = 1$, $p = 0.005$, respectively). The results from comparing these frequency distributions suggest that induction of hyperthermic necrosis requires both MWCNTs and microwave irradiation.

Analyses comparing the frequency distributions of necrosis in mice treated with the two different concentrations of ab-MWCNTs, 0.125 and 0.5 mg/mL, in combination with microwave showed no significant difference. In fact both of these groups (E and H, respectively) have identical frequency distributions. This indicates that the lowest concentration of 0.125 mg/mL was sufficient to produce enough heat to induce hyperthermic necrosis. Previous in vitro studies demonstrated that a concentration of at least 0.1 mg/mL of ab-MWCNTs were necessary to exert cytotoxicity when combined with microwave. Results from that study also indicated that concentrations greater than 0.25 mg/mL of ab-MWCNTs alone induced cytotoxic effects to the cell culture, even without microwave. Thus, this study demonstrates that the lower concentration tested both is effective and also falls into the safe therapeutic window.

No significant difference in the frequency distributions of necrosis was observed between the groups that were injected with ab-MWCNTs with microwave (E and H) and those that were injected with plain MWCNTs with microwave (D and G) at either concentration ($\chi^2 = 1.369$, $df = 1$, $p = 0.2419$ and $\chi^2 = 0.305$, $df = 1$, $p = 0.5808$, respectively). The only difference between these two experimental groups is

the conjugation of anti-PSMA, therefore this comparison evaluates the influence antibody conjugation has on the frequency of necrosis. These results are not surprising, because this construct was not tested in a model bearing a tumor that expresses PSMA in this experiment. Future studies will test the effectiveness of the antibody at targeting the tumor cells.

These data show that intramuscular injection of MWCNTs with concentrations as low as 0.125 mg/mL followed by low levels of microwave irradiation generate enough heat within the tissue to induce muscle cell necrosis. The type of necrosis demonstrated is subtle, localized primarily to the muscle cells immediately adjacent to the MWCNTs. This could be attributed to the small volume of MWCNTs injected, as IM injections should not exceed 0.02 mL. Future studies in a tumor-bearing mouse model could accommodate far larger injection volumes. It is hypothesized that increasing the volume of the MWCNTs and injecting at multiple sites within the tumor will lead to more diffuse necrosis throughout the tissue.

Neutrophilic Infiltration Occurs at the Site of MWCNT Injection

Neutrophilic infiltration was observed surrounding the MWCNTs (Figure 7, red arrows) in all the experimental groups that received IM injections (C-H) and not observed in the control group (A) or the group which received microwave alone (B). The degree of infiltration was variable across all treatment groups with no group demonstrating any noticeable increase over the other. Neutrophilic infiltration can be an indication of cellular death at the site of injection, as these cells are largely responsible for clearing necrotic cellular debris. It can also indicate that the phagocytic cells of the RES system recognize the foreign material and may be attempting to clear the MWCNTs. A notable difference in inflammation between the groups that received microwave in addition to MWCNT injections (D, E, G, and H) would support the hypothesis that these cells were clearing the debris resulting from ablation of the muscle cells, however this was not observed in this study.

Furthermore, a noticeable increase in the groups that received ab-MWCNTs would have shown that the addition of an antibody enhanced RES uptake. This is a common challenge for researchers

incorporating monoclonal antibodies into a targeted therapy, as rapid clearance by the RES system before the application of microwave irradiation would be undesirable. These results did not show a noticeable difference between the experimental groups that included antibody conjugation (C, E, F, and H). These are affirmative results, as they indicate that the method of antibody conjugation does not leave significant portions of the Fc region exposed. Furthermore, neutrophilic infiltration can also indicate that the phagocytic cells of the RES system recognize the foreign material and may be attempting to clear the MWCNTs.

Finally, comparison of the slides from mice sacrificed at 24 hours, 1 week, and 2 weeks seem to demonstrate a decrease in infiltration over time (Figure 9). However, the concentration of MWCNTs remaining in the muscle was consistent across all time points. The culmination of these results indicate that the innate immune system is activated in response to IM injection with MWCNTs. It appears that the phagocytic cells, primarily neutrophils infiltrate the muscle in response to the MWCNTs, and the addition of antibodies or application of microwave do not seem to alter the level of infiltration. While these cells may be effective at clearing cellular debris resulting from associated necrosis, they do not significantly clear the MWCNTs from the site of injection.

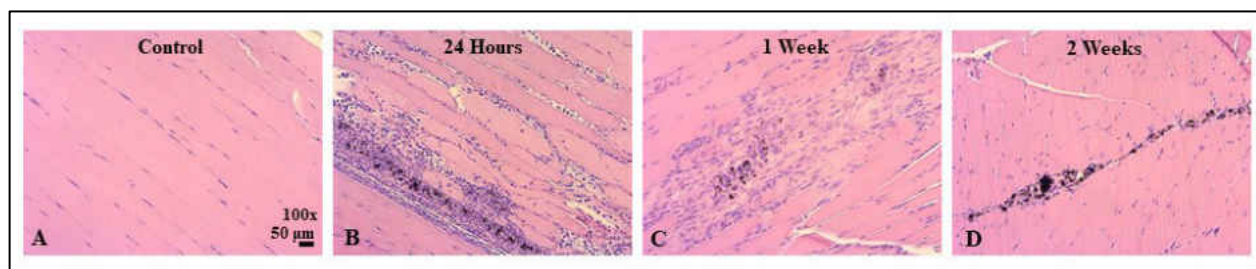


Figure 9. Histology demonstrating decreased inflammation over time. H&E tissue slices demonstrating decreased inflammation at the site of the injection over time as compared to the site in the group that received 0.5 mg/ML CNT plus antibody plus microwave. A) control B) Specimen obtained 24 hours post-treatment, C) 1 week post-treatment, and D) 2 weeks post treatment. 100x total magnification.

IV. MWCNTs are not Evident in the Vital Organs

No evidence of MWCNT or any other pathologies (i.e. inflammation, necrosis, fibrosis, etc.) were observed in any of the H & E stained sections of the vital organs (Figure 10). It is believed that the lack of biodistribution to organs is a function of the route of injection. Numerous studies employing IV

injections have reported histological evidence of accumulation of CNTs in the liver, spleen, and lungs. This is the first study that has performed IM injections, therefore no other comparable reports exist in the literature evaluating this route of exposure. Intra-tumor injections are similar to IM injections, in that both of these routes involve injection into solid tissue, rather than the circulatory system (IV injection) or lymphatic system (SubQ injection). Therefore, it was hypothesized that the biodistribution profile of IM injections would be similar to that of intra-tumor injections reported in other studies, which also reported no evidence of CNTs in these organs. These results confirm that hypothesis.

Additionally, the normal morphology that is observed at all time points demonstrates that the vital organs were not damaged at the tissue level by the whole body microwave irradiation that was administered. This is a cornerstone to the overall therapy that is being proposed: target the cancer cell, while leaving healthy tissue unharmed. The overarching goal for therapies being developed today is to decrease the toxicity to the patient. By demonstrating that the low levels of microwave administered did not cause damage to these organs, these results support continued investigation into this mode of delivering microwave irradiation as part of a combination therapy.

The results from this study also support the hypothesis that IM-injected MWCNTs remain localized to the muscle for up to two weeks, in spite of the robust immune response observed over that time frame. There is no evidence that macrophages and neutrophils are ferrying the MWCNTs through the RES system. This could be an indication that these immune cells are experiencing frustrated phagocytosis, which has been previously reported in the literature.

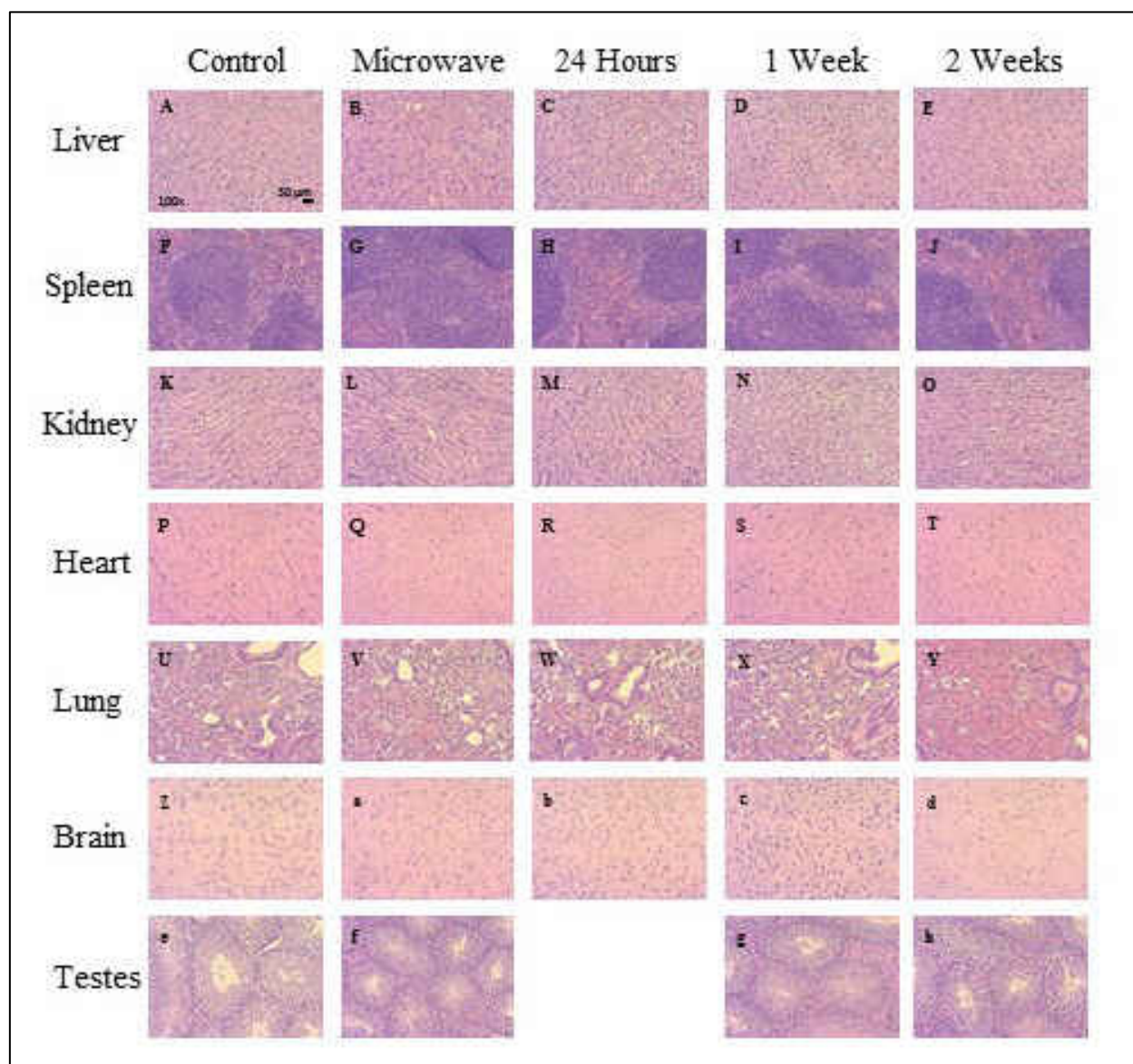


Figure 10. Histology demonstrating organ biodistribution. H&E stained sections of the liver, spleen, kidney, heart, lungs, brain, and testes of the mice that received 0.5 mg/mL ab-MWCNT with microwave at 24 hours (C, H, M, R, W, and b), 1 week (D, I, N, S, X, c, and g), and 2 weeks (E, J, O, T, Y, d, and h) post treatment compared to mice that received no treatment (A, F, K, P, U, Z, and e) and microwave only (B, G, L, Q, V, A, f). 100X Total Magnification.

V. Neutrophils and Macrophages Experience Frustrated Phagocytosis in Zebrafish

The histological studies described above demonstrated neutrophilic infiltration to the muscle at the site of injection. The lack of noticeable biodistribution to the organs of the RES system (liver, spleen, and lungs) indicates that effective phagocytosis may not be occurring. This project thus employed

a study using zebrafish embryos injected with ab-MWCNTs to further understand the interaction occurring between neutrophils and macrophages and ab-MWCNTs.

The neutrophils are the first cells to respond to foreign invaders. Through a process known as diapedesis, they migrate through the endothelial cell lining of the blood vessel from the circulatory system, into the tissue, and arrive at the site of inflammation within 2-4 hours after exposure. They are able to accomplish this rapid immigration because of a unique cellular structure that allows them to take on their characteristic amoeboid shape ⁶⁹. To further understand the neutrophils response to ab-MWCNTs, *Tg(mpx1::gfp)* zebrafish embryos were injected with MWCNTs conjugated to anti-human AlexaFluor647®. Fluorescent confocal microscopy provided live imaging of mounted embryos in which the movement of green fluorescent neutrophils could be viewed in real-time. Because the ab-MWCNTs fluoresce red, this movement can be evaluated spatially in relation to the areas of the embryos concentrated with ab-MWCNTs. All of the embryos that were imaged demonstrated neutrophilic infiltration to areas of

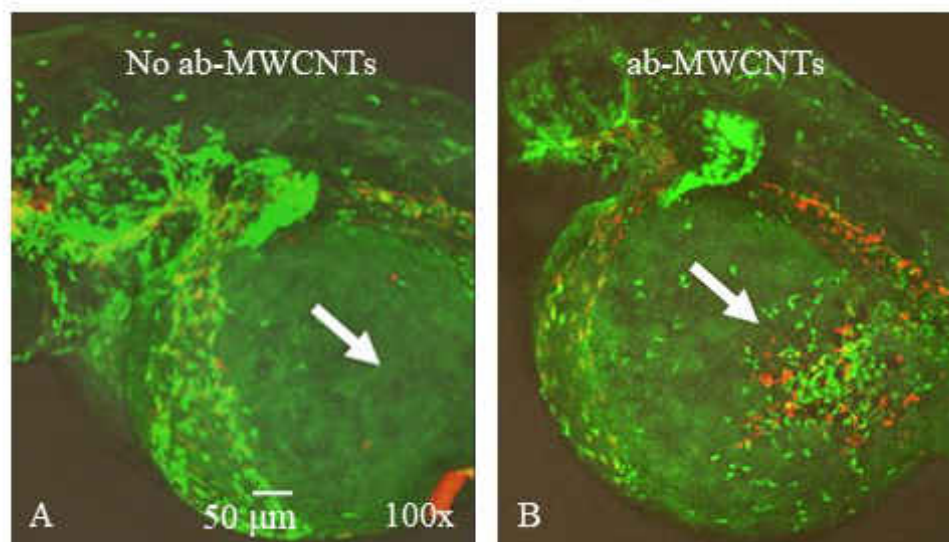
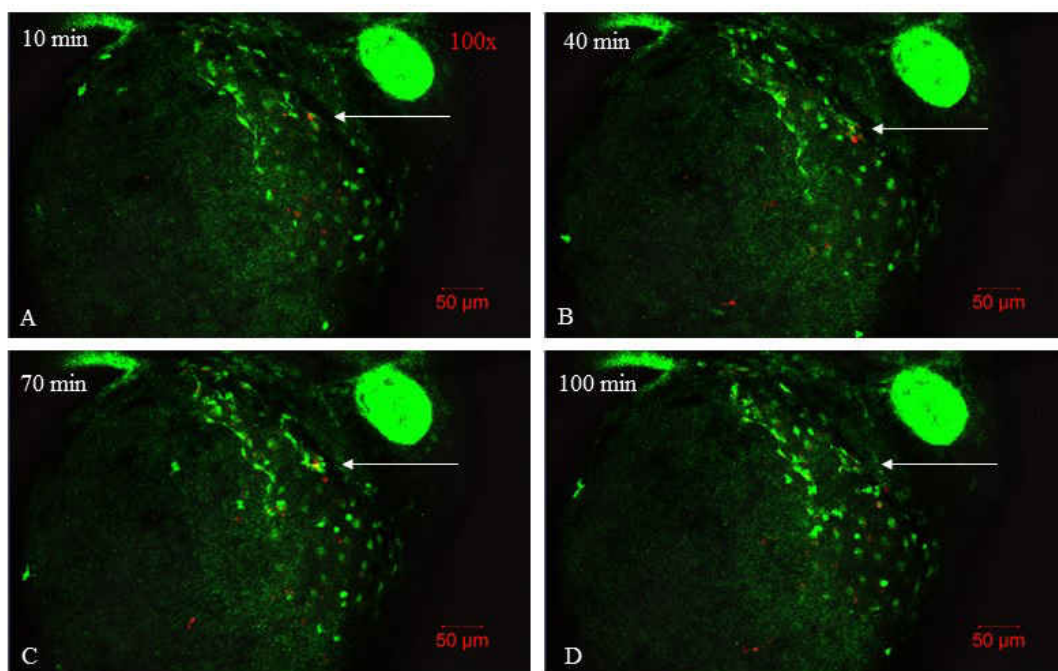


Figure 11. *Tg(mpx1::gfp)* zebrafish embryos demonstrating neutrophilic infiltration specific to ab-MWCNT presence. (A) No ab-MWCNTs are present in the yolk sac along with an absence of neutrophils in this region, serving as a control. (B) A large quantity of ab-MWCNTs are concentrated in this same region of the yolk sac and is accompanied by significant neutrophilic infiltration. Total magnification 100x.

the embryo that were highly concentrated with ab-MWCNTs. These areas were variable between fish, but tended to be most frequently in the yolk sac, tail, and head. Figure 11 illustrates the ab-MWCNT specific migration of the neutrophils seen in the *Tg(mpx1::gfp)* embryos. The embryo on the left (Figure 11-A, white

arrow) has no ab-MWCNTs in the yolk, while the embryo on the right has a high concentration in the same region (Figure 11-B, white arrow). Only the embryo on the right demonstrates a large colony of neutrophils in this same area of the yolk sac. This validates that the yolk sac is not simply a region of the embryo where many neutrophils concentrate and suggests that the neutrophilic infiltration observed is in response to the presence of ab-MWCNTs.

To test the hypothesis that neutrophils would immigrate to the site of ab-MWCNTs, images were taken consecutively over time and compiled into a time-lapse video. The first image was taken about an hour after the injection. In all of the embryos observed, neutrophils had already immigrated to the areas concentrated with ab-MWCNTs. It appears that the majority of neutrophilic infiltration occurred immediately post-injection, and thus the initial migration to the ab-MWCNTs was not captured during the



*Figure 12. Time-lapse demonstrating neutrophil recruitment. Individual time-points from a time-lapse imaging of an *Tg(mpx1::gfp)* transgenic zebrafish embryo injected with MWCNT-AlexaFluor647® at 1 hpi. The white arrow points to a cluster of ab-MWCNTs (red fluorescence). The surrounding green fluorescent neutrophils are moving toward the ab-MWCNTs at 10 (A) and 40 minutes (B). At 70 minutes the neutrophils have reached the ab-MWCNTs and are initiating contact with the cluster (C) and continuing to surround it at 100 minutes (D). Total magnification 100x.*

time-lapse. However, the time-lapse did reveal recruitment of additional neutrophils and the interaction between these cells and ab-MWCNTs. Figure 12 shows specific time-points from a time-lapse analysis of an embryo with ab-MWCNTs concentrated in the yolk sac indicated by the white arrows. Between 10 (Fig.

10-A) and 40 minutes (Fig. 10-B), a group of neutrophils has encircled the cluster of ab-MWCNTs and is moving in closer. By 70 minutes (Fig. 10-C), the neutrophils have covered the cluster and appear to be attempting phagocytosis. At 100 minutes (Fig. 10-D), these same neutrophils are still engaged with the ab-MWCNTs in continued attempt to phagocytize the material. Every embryo that was analyzed demonstrated this response by the neutrophils: Concentration of neutrophils to the region with ab-MWCNTs, maneuvering around a cluster, and eventually closing in with apparent attempted phagocytosis.

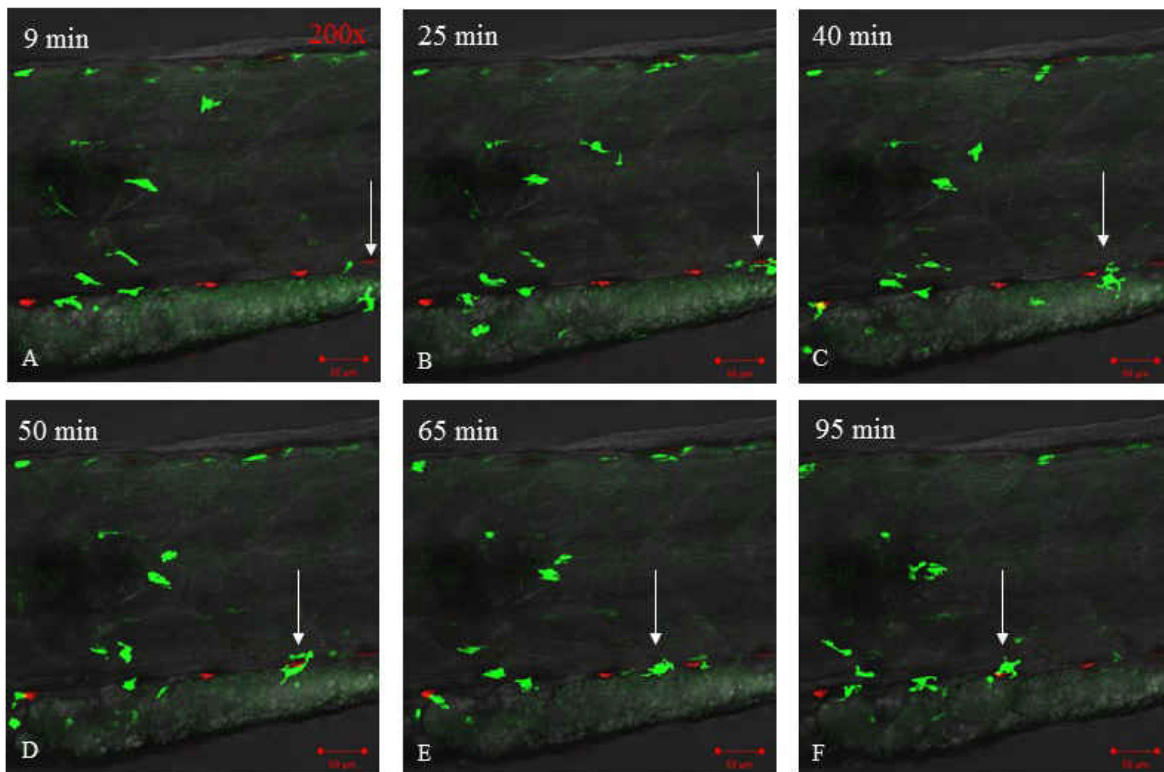


Figure 13. Time-lapse demonstrating attempted macrophage phagocytosis. Individual time-points from a time-lapse imaging of an *mpeg1gfp* transgenic zebrafish embryo injected with MWCNT-AlexaFluor647 at 1 hpi. The white arrows indicate a single macrophage moving from the distal portion of the tail toward a cluster of ab-MWCNTs (red fluorescence) at 9 minutes (A). The macrophage wraps around the cluster after 25 minutes (B) then repeats this movement with the adjacent clusters at 40 minutes (C and D) and 65 minutes (E and F) as it moves along the tail. Total magnification 200X.

The evaluation of the macrophage response to ab-MWCNTs yielded similar findings. To evaluate their response to ab-MWCNTs, *Tg(mpeg1::gfp)* embryos that have macrophages that express GFP were used and imaged in the same manner as described above. Generally, macrophages take longer to immigrate to the site of inflammation and are the last to leave, as their primary function is to clean up cellular debris that results from the inflammatory process⁶⁹. It was hypothesized that because these cells

are slower to arrive, the time-lapse imaging would be able to capture their initial migration. However, similar to the neutrophil analyses, macrophages were already in proximity to the ab-MWCNTs within the hour it took to mount the embryos. The increased size and slower movement in comparison to neutrophils, did make visualization of the macrophage response to ab-MWCNTs more clear. Figure 13 shows specific time-points from a time-lapse analysis of an embryo with ab-MWCNTs concentrated in the tail. The white arrow follows a single macrophage as it moves toward a single cluster of ab-MWCNTs at 9 minutes (Fig. 13-A) and wraps itself around it at 25 minutes (Fig.13-B). This macrophage then leaves and moves on toward an adjacent cluster at 40 minutes (Fig. 13-C) and again wraps its amoeboid shape around it at 50 minutes (Fig. 13-D). For a third time, it repeats this motion at 65 and 95 minutes (Fig. 13-E,F).

It remains unclear whether the neutrophils and macrophages were successful in clearing the material. It is challenging to visualize the ab-MWCNTs once they have been engulfed within the lysosomes of these phagocytic cells, as the enzymes within these compartments likely rapidly degrade the fluorescent dyes along with denaturation of the antibody. One indication that phagocytosis was successful would be to witness a decrease in the concentration of ab-MWCNT concentration to the original region of the embryo or redistribution to other areas, along with a receding of the WBCs that infiltrated. This was evaluated by repeating imaging surviving fish at 24 hours and 72 hours post injection. These images revealed that both the neutrophils and macrophages remained localized to the original areas of ab-MWCNT concentration for up to 72 hours. This suggests that these cells were, in fact, experiencing frustrated phagocytosis and were unable to clear the ab-MWCNTs.

VI. Effects of Microwave on Mice

During the microwave power trials, all mice tolerated 500 J and 750 J of energy. They displayed normal behavior and exhibited no evidence of physical distress or injury related to treatment

during the 48 hour observation period. The decision to proceed with the experiments was based on these results. The 48 hour outcomes for mice in the experimental groups that received microwave irradiation were consistent with those in the power trial. However at 3 days post treatment, some mice began to experience tail and right hind foot sores consistent with surface burns (Figure 11). Of the mice that were sacrificed at 2 weeks post treatment, 93% of those who experienced microwave irradiation developed sores by day 9. These mice were still active and displayed normal social behavior and biological functions (eating, drinking, defecating, etc.) comparable to the mice who received no treatment. They displayed no overt signs of pain or distress.

This is most likely a limitation of the experimental design as opposed to a biological problem with the proposed treatment. First, it is hypothesized that the sores emerged on the tail and feet due to the low water content in these areas which are composed primarily of skin and bone and very little fat. Water efficiently absorbs microwaves due to its dipolar structure⁷⁴. What little water was present in these regions likely evaporated rapidly. Additionally, positioning the mice in the microwave in the prone position with the tail wrapped around its body exposed the tail and right hind leg. This may have prevented the mice's body from insulating the exposed regions (Figure 12). Finally, the application of whole body microwave did not provide a way to direct the waves away from these vulnerable areas. The microwave setup should be further optimized before any future studies are attempted. One alternative could be to use a microwave source which directs the waves to a target area making the energy concentration more localized. Another

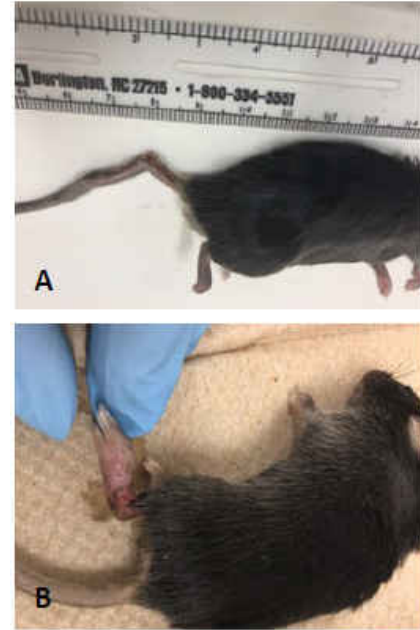


Figure 14. Microwave-induced lesions in mice. Examples show lesions on the tail (A) and foot (B).



Figure 15. Mouse positioning for microwave irradiation.

alternative is to develop a shield for the vulnerable areas out of a substance that reflects microwaves. Finally, tail-less rodent model could be chosen so long as one can ensure that the feet could be shielded by the body.

CHAPTER 4

CONCLUSION

I. A Novel Therapy

The proposed treatment that was evaluated in this study is entirely novel in several ways. First, the method of conjugating the antibody to the surface of the MWCNTs was developed by this lab. Second, while anti-PSMA has been used to successfully treat prostate cancer, it has never been conjugated to carbon nanotubes. Finally, possibly most notably, no one has ever evaluated microwave-induced heating of carbon nanotubes as a possible cancer ablation therapy in mice.

The goal of this project was to evaluate this novel therapy by testing three hypotheses. The first was that IM injected ab-MWCNTs followed by microwave irradiation can cause hyperthermic ablation in mice. Histological examination demonstrated hyperthermic necrosis only in the groups that received both MWCNTs and microwave irradiation. Importantly, the level of microwave that successfully heated the MWCNTs was low enough as to not cause overt toxicity to the host. The second hypothesis was that ab-MWCNTs would remain localized at the site of injection. Histological examination of the muscle at the site of injection and the vital organs of groups sacrificed at different time-points confirmed that the MWCNTs remained in the muscle for at least 2 weeks and did not redistribute to other organs during that time frame. Furthermore, the normal morphology observed in every specimen indicates that microwave alone did not cause obvious tissue damage. These results have been corroborated by a collaborating lab analyzing serum biomarkers that are indicators of organ-specific toxicity. The final hypothesis was that the innate immune system would mount an inflammatory response against the ab-MWCNTs. This was observed histologically by neutrophilic infiltration of the muscle at the site of injection and through florescent time-lapse images that showed macrophages and neutrophils attempting phagocytosis of the ab-MWCNTs. While these

experiments yielded valuable information, they also illuminated new challenges and further evaluations that could be endeavored.

II. Further Evaluation of Results

Histopathology: While evidence of necrosis is present, the degree was very subtle. It is standard to perform an H&E stain to evaluate changes in morphology as the first course of action. The suspected necrosis could be further evaluated by taking additional section and applying a special stain more sensitive to detecting necrosis. A modified staining method to detect lactate dehydrogenase (LDH) has been described for the enhanced detection of thermally damaged tissue ⁷⁵. Other histochemical stains could also be used to further evaluate the immune response demonstrated at the site of injection. It is unclear whether the phagocytic cells are capable of successfully performing phagocytosis of the MWCNTs. One hallmark of frustrated phagocytosis is the continued production of reactive oxidative species (ROS) ³⁰. The released ROS then acts upon the surrounding cells causing lipid peroxidation and the formation of 4-Hydroxynonenal (4HNE). Histochemical stains which detect 4HNE could yield more information about the inflammatory activities of the immune cells present at the site of inflammation ⁷⁶.

Biodistribution: Because the MWCNTs are by definition nanomaterials, it is plausible that they are in fact broken down and distributed to various organs at a level that is not detectable by light microscopy. A more sensitive approach to search for evidence of MWCNT migration to tissue is to also conjugate a radioactive isotope to the surface along with the antibody. The organs can then be homogenized at necropsy and analyzed via dosimetry for levels of radioactivity ⁴³. Toxicity can also be measured using serum clinical assays. Another collaborator, is currently analyzing serum samples taken at the time of necropsy for the following biomarkers which are indicators of organ damage: Creatinine (kidney), AST and ALT (liver), albumin and total protein (inflammation). Preliminary results from these studies indicate no significant differences in levels of these analytes between the groups. This correlates with the histopathological results obtained by this study, further indicating that the experiments did not cause

toxicity to the mice and that the inflammation was not systemic. This lab is also performing RNA expression assays on the liver, kidney, and brain for the following proteins associated with inflammation: Interleukin 1- β , Interleukin-6, nuclear factor kappa-light-chain-enhancer of activated B cells (NF κ B), Prostaglandin-endoperoxide synthase 2 (PTGS2), and tumor necrosis factor (TNF). These assays will shed more light on the inflammatory state of these organs at the time of necropsy ⁷⁷.

III. Further Modification of MWCNTs

Increase Biocompatibility: It should be explored whether further efforts should be made to improve the biocompatibility of the MWCNTs. A certain level of dispersability should be achieved if the ab-MWCNTs are to reach the target antigen. Ideally, the nanotubes would stay long enough to be heated and cause tumor necrosis and then be cleared through RES system and eventually excreted through the biliary or urinary tract. This study demonstrated that this compound in its current state remains localized at the site of injection. This seems to ultimately lead to less organ biodistribution and thus less toxicity than other more dispersible CNTs. However, it is possible that the current level of biocompatibility will inhibit the movement necessary for the nanomaterial to maneuver through the tumor microenvironment to reach its target. Also, it is unknown what the long-term damage is of leaving this type of nanomaterial in the body indefinitely. Methods to further functionalize the surface of the walls making them more hydrophilic have may improve the efficacy of this proposed treatment. Other methods include bathing the nanotubes in a strong acid to remove impurities ⁷⁸, further functionalization with glucosamine⁵⁰, and the covalent addition of polyethylene glycol (PEG)⁵⁸.

Alternative Antibody Conjugation: The Fc portion of antibodies are the effector regions of the molecule. Interaction with proteins and receptors are a point of initiation of a number of cascades involved the immune response, including macrophage clearance and complement activation. Whenever conjugating an antibody to a compound, the goal is to anchor the Fc portion to the wall to minimize these effects and to allow the Fab region to extend outward to enhance the likelihood it will bind to the target antigen. The current form of conjugation interacts with the N-terminus region of the antibody. Antibodies

are composed of multiple protein subunits, each with a C-terminus and an N-terminus. This means that the antibody can attach at multiple points throughout the protein. It may be worthwhile to explore forming a bond between the carbohydrate groups that are concentrated in the Fc portion and the carboxyl groups on the functionalized MWCNTs. Another option may be to coat the surface of the MWCNTs with biotin and use a commercially prepared antibody with streptavidin already on the Fc region. The biotin/streptavidin interaction forms a strong covalent bond ⁶⁹.

Localized Inflammation: It is important to note that localized inflammation at a tumor site can also be a benefit. Activation of complement from the antibody coated MWCNTs may in fact aid in the cytotoxic killing of the tumor cells. Furthermore, if the immune cells are in fact capable of performing complete phagocytosis, then this will help with clearing the cellular debris and wound healing post hyperthermic ablation. Neutrophils and macrophages also act as antigen presenting cells (APC), processing antigens that are engulfed and presenting them to lymphocytes for recruitment of the adaptive immune system. It is possible that the cleanup efforts by the APCs of the necrotic cancer cells may lead to antigen presentation of specific cancer antigens and a heightened adaptive immune response to the cancer. Too much inflammation can be detrimental, however. Over-activation of inflammatory cascades can lead to a cytokine storm and shock. This has been seen widely in current therapies aimed at using one's own immune system to fight cancer. Additionally, inflammatory cells within tumors have been demonstrated to aid in cancer metastasis ⁷⁹. The extent of immune involvement which aid or conversely is detrimental in combating cancer involves many mechanisms that have yet to be elucidated.

IV. Conclusion

The promising results obtained are at the ground level of investigating this combination therapy as a possible treatment for cancer. The next step is to evaluate the role that antibody conjugation plays in making the proposed therapy more effective at targeting cancer cells directly. To evaluate the role that anti-PSMA plays in improving this tumor ablation therapy, experiments must be performed in a

prostate tumor-bearing model. Further functionalization to improve biocompatibility of the ab-MWCNTs and the microwave settings may require more optimization first.

Cancer therapy research is focused on finding a treatment that selectively kills cancer cells while leaving healthy cells unharmed. The use of antibodies as a form of targeting cancers with drug payloads or for targeted ablative therapies has proven to be effective for a number of cancers. The incorporation of nanomaterials has also broadened the horizons for unique opportunities to address the fight against cancer. Carbon nanotubes are a promising candidate because their surface chemistry allows for the conjugation of antibodies and also has the capacity for super-heating under microwave irradiation. This is especially useful because microwaves penetrate deeper than traditional NIR and provide more uniform heating. These various elements make the proposed treatment evaluated by this study unique in its class. This study proves the concept that low levels of microwave irradiation can penetrate mammalian tissue and, when combined with MWCNTs, cause cell ablation. The use ab-MWCNTs and microwave to deliver targeted cancer cell ablation is a viable candidate for incorporation into existing combination therapies and is worth exploring further.

REFERENCES

1. Cancer Facts and Figures. 2018. In: Society AC, editor. Atlanta, GA.
2. Stewart B, and Wild C. 2014. World Cancer Report 2014. Lyon. France: International Agency for Research on Cancer.
3. National Cancer Institute: Cancer MoonshotSM – Funding by Research Category. 2018. National Cancer Institute; [accessed 2019 April 5]. <https://www.cancer.gov/about-nci/budget/fact-book/cancer-moonshot/moonshot-research-categories>.
4. DeVita VT, Jr., Chu E. 2008. A history of cancer chemotherapy. *Cancer Res.* 68(21):8643-8653.
5. Chari RVJ. 2008. Targeted Cancer Therapy: Conferring Specificity to Cytotoxic Drugs. *Acc Chem Res.* 41(1):98-107.
6. Ng AK, Kenney LB, Gilbert ES, Travis LB. 2010. Secondary malignancies across the age spectrum. *Semin Radiat Oncol.* 20(1):67-78.
7. Connell PP, Hellman S. 2009. Advances in Radiotherapy and Implications for the Next Century: A Historical Perspective. *Cancer Res.* 69(2):383-392.
8. National Cancer Institute: Hyperthermia in Cancer Treatment. 2011. National Cancer Institute; [accessed 2019 April 5]. <https://www.cancer.gov/about-cancer/treatment/types/surgery/hyperthermia-fact-sheet>.
9. Glazer ES, Curley SA. 2011. The ongoing history of thermal therapy for cancer. *Surg Oncol Clin N Am.* 20(2):229-235, vii.
10. Sharma A, Abtin F, Shepard J-AO. 2012. Image-Guided Ablative Therapies for Lung Cancer. *Radiat Clin N Am.* 50(5):975-999.
11. Little MW, Chung D, Boardman P, Gleeson FV, Anderson EM. 2013. Microwave ablation of pulmonary malignancies using a novel high-energy antenna system. *Cardiovasc Intervent Radiol.* 36(2):460-465.
12. Liu Y, Zheng Y, Li S, Li B, Zhang Y, Yuan Y. 2013. Percutaneous microwave ablation of larger hepatocellular carcinoma. *Clin Radiol.* 68(1):21-26.

13. Yan TD, King J, Sjarif A, Glenn D, Steinke K, Morris DL. 2006. Percutaneous radiofrequency ablation of pulmonary metastases from colorectal carcinoma: prognostic determinants for survival. *Ann Surg Oncol.* 13(11):1529-1537.
14. Nagayama A, Ellisen LW, Chabner B, Bardia A. 2017. Antibody-Drug Conjugates for the Treatment of Solid Tumors: Clinical Experience and Latest Developments. *Target Oncol.* 12(6):719-739.
15. Sun T, Zhang YS, Pang B, Hyun DC, Yang M, Xia Y. 2014. Engineered nanoparticles for drug delivery in cancer therapy. *Angew Chem Int Ed Engl.* 53(46):12320-12364.
16. Ventola C. 2017. Progress in Nanomedicine: Approved and Investigational Nanodrugs. *P T.* 42(12):13.
17. von Roemeling C, Jiang W, Chan CK, Weissman IL, Kim BYS. 2017. Breaking Down the Barriers to Precision Cancer Nanomedicine. *Trends Biotechnol.* 35(2):159-171.
18. D'Mello SR, Cruz CN, Chen ML, Kapoor M, Lee SL, Tyner KM. 2017. The evolving landscape of drug products containing nanomaterials in the United States. *Nat Nanotechnol.* 12(6):523-529.
19. Tran S, DeGiovanni PJ, Piel B, Rai P. 2017. Cancer nanomedicine: a review of recent success in drug delivery. *Clin Transl Med.* 6(1):44.
20. Lancet JE, Uy GL, Cortes JE, Newell LF, Lin TL, Ritchie EK, Stuart RK, Strickland SA, Hogge D, Solomon SR et al. 2016. Final results of a phase III randomized trial of CPX-351 versus 7+3 in older patients with newly diagnosed high risk (secondary) AML. *J Clin Oncol.* 34(15_suppl):7000-7000.
21. Shore ND, Chu F, Moul J, Saltzstein D, Concepcion R, McLane JA, Atkinson S, Yang A, Crawford ED. 2017. Polymer-delivered subcutaneous leuprolide acetate formulations achieve and maintain castrate concentrations of testosterone in four open-label studies in patients with advanced prostate cancer. *BJU Int.* 119(2):239-244.
22. Maier-Hauff K, Ulrich F, Nestler D, Niehoff H, Wust P, Thiesen B, Orawa H, Budach V, Jordan A. 2011. Efficacy and safety of intratumoral thermotherapy using magnetic iron-oxide nanoparticles combined with external beam radiotherapy on patients with recurrent glioblastoma multiforme. *J Neurooncol.* 103(2):317-324.

23. Medical Device Network. MagForce to study NanoTherm therapy for prostate cancer in US. 2019.
24. Rastogi V, Yadav P, Bhattacharya SS, Mishra AK, Verma N, Verma A, Pandit JK. 2014. Carbon nanotubes: an emerging drug carrier for targeting cancer cells. *J Drug Deliv.* 2014:670815.
25. Shi D, Mi G, Webster TJ. 2016. The Synthesis, Application, and Related Neurotoxicity of Carbon Nanotubes. In: Jiang X, Gao H, editors. *Neurotoxicity of Nanomaterials and Nanomedicine.* Elsevier Science. p. 259-284.
26. Sayes CM, Liang F, Hudson JL, Mendez J, Guo W, Beach JM, Moore VC, Doyle CD, West JL, Billups WE et al. 2006. Functionalization density dependence of single-walled carbon nanotubes cytotoxicity in vitro. *Toxicol Lett.* 161(2):135-142.
27. Liu Z, Tabakman SM, Chen Z, Dai H. 2009. Preparation of carbon nanotube bioconjugates for biomedical applications. *Nat Protoc.* 4(9):1372-1382.
28. Kaufmann A, Hampel S, Rieger C, Kunhardt D, Schendel D, Fussel S, Schwenzer B, Erdmann K. 2017. Systematic evaluation of oligodeoxynucleotide binding and hybridization to modified multi-walled carbon nanotubes. *J Nanobiotechnol.* 15(1):53.
29. Poland CA, Duffin R, Kinloch I, Maynard A, Wallace WA, Seaton A, Stone V, Brown S, Macnee W, Donaldson K. 2008. Carbon nanotubes introduced into the abdominal cavity of mice show asbestos-like pathogenicity in a pilot study. *Nat Nanotechnol.* 3(7):423-428.
30. Boyles MS, Young L, Brown DM, MacCalman L, Cowie H, Moisala A, Smail F, Smith PJ, Proudfoot L, Windle AH et al. 2015. Multi-walled carbon nanotube induced frustrated phagocytosis, cytotoxicity and pro-inflammatory conditions in macrophages are length dependent and greater than that of asbestos. *Toxicol In Vitro.* 29(7):1513-1528.
31. Salvador-Morales C, Flahaut E, Sim E, Sloan J, H. Green ML, Sim RB. 2006. Complement activation and protein adsorption by carbon nanotubes. *J Mol Immunol.* 43(3):193-201.
32. Di Giorgio ML, Di Bucchianico S, Ragnelli AM, Aimola P, Santucci S, Poma A. 2011. Effects of single and multi walled carbon nanotubes on macrophages: cyto and genotoxicity and electron microscopy. *Mutat Res.* 722(1):20-31.

33. Meng J, Yang M, Jia F, Xu Z, Kong H, Xu H. 2011. Immune responses of BALB/c mice to subcutaneously injected multi-walled carbon nanotubes. *Nanotoxicology*. 5(4):583-591.
34. Ding L, Stilwell J, Zhang T, Elboudwarej O, Jiang H, Selegue JP, Cooke PA, Gray JW, Chen FF. 2005. Molecular Characterization of the Cytotoxic Mechanism of Multiwall Carbon Nanotubes and Nano-Onions on Human Skin Fibroblast. *Nano Letters*. 5(12):2448-2464.
35. Yang S-T, Wang X, Jia G, Gu Y, Wang T, Nie H, Ge C, Wang H, Liu Y. 2008. Long-term accumulation and low toxicity of single-walled carbon nanotubes in intravenously exposed mice. *Toxicology Letters*. 181(3):182-189.
36. Lacerda L, Ali-Boucetta H, Herrero MA, Pastorin G, Bianco A, Prato M, Kostarelos K. 2008. Tissue histology and physiology following intravenous administration of different types of functionalized multiwalled carbon nanotubes. *Nanomedicine*. 3(2):149-161.
37. Schipper ML, Nakayama-Ratchford N, Davis CR, Wong Shi Kam N, Chu P, Zhuang L, Xiaoming S, Hongjie D, Gambhir SS. 2008. A pilot toxicology study of single-walled carbon nanotubes in a small sample of mice. *Nature Nanotechnology*. 3(4):216-221.
38. Wu W, Li R, Bian X, Zhu Z, Ding D, Li X, Jia Z, Jiang X, Hu Y. 2009. Covalently Combining Carbon Nanotubes with Anticancer Agent: Preparation and Antitumor Activity. *ACS Nano*. 3(9):2740-2750.
39. Li J, Pant A, Chin CF, Ang WH, Menard-Moyon C, Nayak TR, Gibson D, Ramaprabhu S, Panczyk T, Bianco A et al. 2014. In vivo biodistribution of platinum-based drugs encapsulated into multi-walled carbon nanotubes. *Nanomedicine*. 10(7):1465-1475.
40. Bhirde AA, Chikkaveeraiah BV, Srivatsan A, Niu G, Jin AJ, Kapoor A, Wang Z, Patel S, Patel V, Gorbach AM et al. 2014. Targeted Therapeutic Nanotubes Influence the Viscoelasticity of Cancer Cells to Overcome Drug Resistance. *ACS Nano*. 8(5):4177-4189.
41. Datir SR, Das M, Singh RP, Jain S. 2012. Hyaluronate tethered, "smart" multiwalled carbon nanotubes for tumor-targeted delivery of doxorubicin. *Bioconj Chem*. 23(11):2201-2213.

42. Liu Z, Cai W, He L, Nakayama N, Chen K, Sun X, Chen X, Dai H. 2007. In vivo biodistribution and highly efficient tumour targeting of carbon nanotubes in mice. *Nat Nanotechnol.* 2(1):47-52.
43. McDevitt MR, Chattopadhyay D, Kappel BJ, Jaggi JS, Schiffman SR, Antczak C, Njardarson JT, Brentjens R, Scheinberg DA. 2007. Tumor targeting with antibody-functionalized, radiolabeled carbon nanotubes. *J Nucl Med.* 48(7):1180-1189.
44. Yang F, Hu, J. 2009. Pilot study of targeting magnetic carbon nanotubes to lymph nodes. *Nanomedicine.* 4(3):13.
45. Burke A, Ding X, Singh R, Kraft RA, Levi-Polyachenko N, Rylander MN, Szot C, Buchanan C, Whitney J, Fisher J et al. 2009. Long-term survival following a single treatment of kidney tumors with multiwalled carbon nanotubes and near-infrared radiation. *Proc Natl Acad Sci U S A.* 106(31):12897-12902.
46. Podesta JE, Al-Jamal KT, Herrero MA, Tian B, Ali-Boucetta H, Hegde V, Bianco A, Prato M, Kostarelos K. 2009. Antitumor activity and prolonged survival by carbon-nanotube-mediated therapeutic siRNA silencing in a human lung xenograft model. *Small.* 5(10):1176-1185.
47. Dumortier H, Lacotte S, Pastorin G, Marega R, Wu W, Bonifazi D, Briand J-P, Prato M, Muller S, Bianco A. 2006. Functionalized Carbon Nanotubes Are Non-Cytotoxic and Preserve the Functionality of Primary Immune Cells. *Nano Letters.* 6(7):1522-1528.
48. Yang S-T, Wang Y-W, Liu J-H, Wang H. 2012. Biodistribution of multi-walled carbon nanotubes functionalized by hydroxyl terminated poly(ethylene glycol) in mice. *J Radioanal Nucl Ch.* 295(2):1181-1186.
49. Singh R, Pantarotto D, Lacerda L, Pastorin G, Klumpp C, Prato M, Bianco A, Kostarelos K. 2006. Tissue biodistribution and blood clearance rates of intravenously administered carbon nanotube radiotracers. *Proc Natl Acad Sci U S A.* 103(9):3357-3362.
50. Guo J, Zhang X, Li Q, Li W. 2007. Biodistribution of functionalized multiwall carbon nanotubes in mice. *Nucl Med Biol.* 34(5):579-583.

51. Liang X, Shang W, Chi C, Zeng C, Wang K, Fang C, Chen Q, Liu H, Fan Y, Tian J. 2016. Dye-conjugated single-walled carbon nanotubes induce photothermal therapy under the guidance of near-infrared imaging. *Cancer Lett.* 383(2):243-249.
52. Fisher JW, Sarkar S, Buchanan CF, Szot CS, Whitney J, Hatcher HC, Torti SV, Rylander CG, Rylander MN. 2010. Photothermal response of human and murine cancer cells to multiwalled carbon nanotubes after laser irradiation. *Cancer Res.* 70(23):9855-9864.
53. Ghosh S, Dutta S, Gomes E, Carroll D, D'Agostino R, Olson J, Guthold M, Gmeiner WH. 2009. Increased Heating Efficiency and Selective Thermal Ablation of Malignant Tissue with DNA-Encased Multiwalled Carbon Nanotubes. *ACS Nano.* 3(9):2667-2673.
54. Kam NWS, O'Connell M, Wisdom JA, Dai H. 2005. Carbon nanotubes as multifunctional biological transporters and near-infrared agents for selective cancer cell destruction. *Proc Natl Acad Sci USA.* 102(33):11600-11605.
55. Heister E, Neves V, Tilmaciu C, Lipert K, Beltrán VS, Coley HM, Silva SRP, McFadden J. 2009. Triple functionalisation of single-walled carbon nanotubes with doxorubicin, a monoclonal antibody, and a fluorescent marker for targeted cancer therapy. *Carbon.* 47(9):2152-2160.
56. Li R, Wu Ra, Zhao L, Wu M, Yang L, Zou H. 2010. P-Glycoprotein Antibody Functionalized Carbon Nanotube Overcomes the Multidrug Resistance of Human Leukemia Cells. *ACS Nano.* 4(3):1399-1408.
57. Liu Z, Tabakman S, Welsher K, Dai H. 2009. Carbon Nanotubes in Biology and Medicine: In vitro and in vivo Detection, Imaging and Drug Delivery. *Nano Res.* 2(2):85-120.
58. Khandare JJ, Jalota-Badhwar A, Satavalekar SD, Bhansali SG, Aher ND, Kharas F, Banerjee SS. 2012. PEG-conjugated highly dispersive multifunctional magnetic multi-walled carbon nanotubes for cellular imaging. *Nanoscale.* 4(3):837-844.
59. Yuksel M, Colak DG, Akin M, Cianga I, Kukut M, Medine EI, Can M, Sakarya S, Unak P, Timur S et al. 2012. Nonionic, water self-dispersible "hairy-rod" poly(p-phenylene)-g-poly(ethylene glycol)

- copolymer/carbon nanotube conjugates for targeted cell imaging. *Biomacromolecules*. 13(9):2680-2691.
60. Pan J, Li F, Choi JH. 2017. Single-walled carbon nanotubes as optical probes for bio-sensing and imaging. *J Mater Chem B*. 5(32):6511-6522.
61. Jeyamohan P, Hasumura T, Nagaoka Y, Yoshida Y, Maekawa T, Kumar DS. 2013. Accelerated killing of cancer cells using a multifunctional single-walled carbon nanotube-based system for targeted drug delivery in combination with photothermal therapy. *Int J Nanomedicine*. 8:2653-2667.
62. Robinson AD. 2012. *The Incorporation of Nanomaterials in Cancer Therapy*. [Statesboro, GA]: Georgia Southern University.
63. Beckler B, Cowan A, Farrar N, Murawski A, Robinson A, Diamanduros A, Scarpinato K, Sittaramane V, Quirino RL. 2018. Microwave Heating of Antibody-functionalized Carbon Nanotubes as a Feasible Cancer Treatment. *Biomed Phys Eng Express*. 4(4):045025.
64. Bernacki Kurt D, Fields Kristina L, Roh Michael H. 2013. The utility of PSMA and PSA immunohistochemistry in the cytologic diagnosis of metastatic prostate carcinoma. *Diagn Cytopathol*. 42(7):570-575.
65. Thapa R, Wilson GD. 2016. The Importance of CD44 as a Stem Cell Biomarker and Therapeutic Target in Cancer. *Stem Cells Int*. 2016:2087204.
66. Davis MI, Bennett MJ, Thomas LM, Bjorkman PJ. 2005. Crystal structure of prostate-specific membrane antigen, a tumor marker and peptidase. *Proc Natl Acad Sci U S A*. 102(17):5981-5986.
67. Ghosh A, Heston WD. 2004. Tumor target prostate specific membrane antigen (PSMA) and its regulation in prostate cancer. *J Cell Biochem*. 91(3):528-539.
68. Ristau BT, O'Keefe DS, Bacich DJ. 2014. The prostate-specific membrane antigen: Lessons and current clinical implications from 20 years of research. *Urol Oncol*. 32(3):272-279.
69. Stevens CD, Miller LE. 2017. *Clinical Immunology and Serology*. Philadelphia, PA: F. A. Davis Company.

70. Song HK, Hwang DY. 2017. Use of C57BL/6N mice on the variety of immunological researches. *Lab Anim Res.* 33(2):119-123.
71. Bryant CD. 2011. The blessings and curses of C57BL/6 substrains in mouse genetic studies. *Ann N Y Acad Sci.* 1245:31-33.
72. Mosca F, Tritto E, Muzzi A, Monaci E, Bagnoli F, Iavarone C, O'Hagan D, Rappuoli R, De Gregorio E. 2008. Molecular and cellular signatures of human vaccine adjuvants. *Proc Natl Acad Sci U S A.* 105(30):10501-10506.
73. Theodora: Basic Bi methodology for Laboratory Mice. 2004. [accessed 2019 April 14]. https://theodora.com/rodent_laboratory/injections.html.
74. Vázquez E, Prato M. 2009. Carbon Nanotubes and Microwaves: Interactions, Responses, and Applications. *ACS Nano.* 3(12):3819-3824.
75. Sherwood ME, Flotte TJ. 2007. Improved staining method for determining the extent of thermal damage to cells. *Lasers Surg Med.* 39(2):128-131.
76. Liou GY, Storz P. 2015. Detecting reactive oxygen species by immunohistochemistry. *Methods Mol Biol.* 1292:97-104.
77. Gato E, Mixson A, Clark C, Kusi Y. Forthcoming 2019. Preliminary results from clinical assays performed in collaboration with "Evaluating the effects of antibody-conjugated multi-walled carbon nanotubes in combination with microwave irradiation.". Statesboro, GA: Georgia Southern University.
78. Adenuga AA, Truong L, Tanguay RL, Remcho VT. 2013. Preparation of water soluble carbon nanotubes and assessment of their biological activity in embryonic zebrafish. *Int J Biomed Nanosci Nanotechnol.* 3(1-2):38-51.
79. Janssen LME, Ramsay EE, Logsdon CD, Overwijk WW. 2017. The immune system in cancer metastasis: friend or foe? *J Immunother Cancer.* 5(1):79.